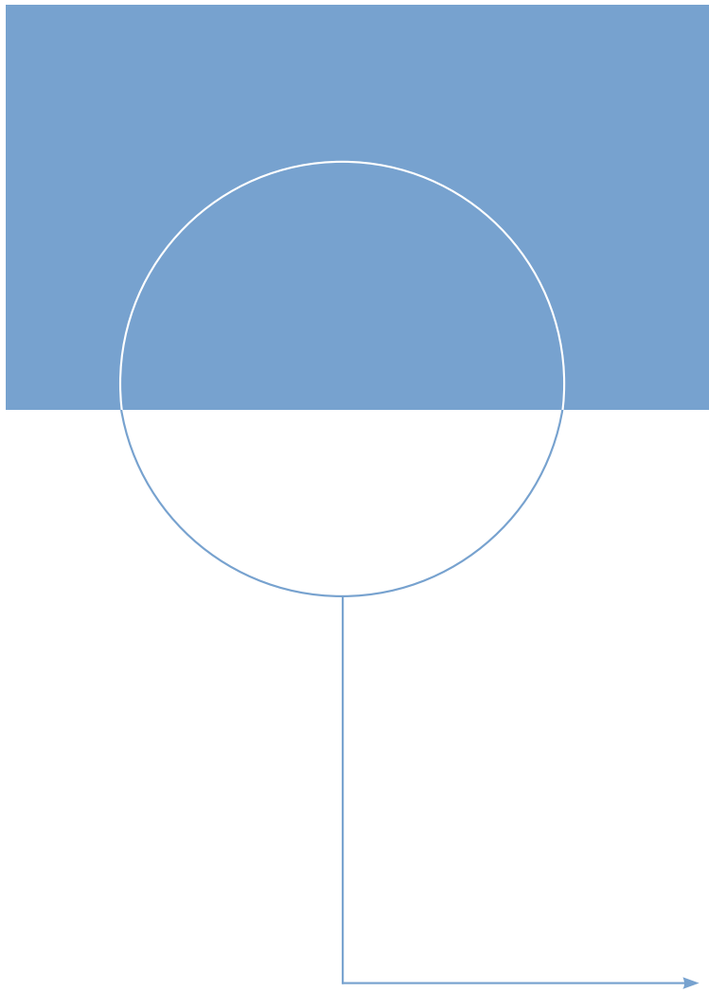

Master's thesis

2020

Hayden Joe

NTNU
Norwegian University of
Science and Technology
Faculty of Engineering
Department of Civil and Environmental Engineering

Hayden Joe

Verdal Port Landslide: Slope Stability Back Analysis from CPTU and Finite Element Modelling

June 2020

NTNU
Norwegian University of
Science and Technology

NTNU
Norwegian University of
Science and Technology

NTNU

Norwegian University of
Science and Technology

Verdal Port Landslide: Slope Stability Back Analysis from CPTU and Finite Element Modelling

Hayden Joe

Geotechnics and Geohazards Master's Thesis: TBA4900
Submission date: June 2020
Supervisor: Jean-Sebastian L'Heureux, NGI
Co-supervisor: Ragnar Moholdt, NGI, Ana Priscilla Paniagua Lopez, NTNU

Norwegian University of Science and Technology
Department of Civil and Environmental Engineering

Preface

This paper was developed during the spring semester of 2020. It stands as a one-semester Master's thesis to fulfil the requirements for TBA4900 as part of the MSc Geotechnics and Geohazards program in the Department of Civil and Environmental Engineering at the Norwegian University of Science and Technology. This paper builds upon the project conducted during TBA4510 and relevant pre-analysis material has been incorporated in this work. The supervisors for this project were Ragnar Moholdt and Jean-Sebastien L'Heureux from the Norwegian Geotechnical Institute and Ana Priscilla Paniagua López who represents both the Norwegian University of Science and Technology and the Norwegian Geotechnical Institute.

My goal for this project was to investigate a geotechnical case study to gain practical knowledge about the processes and uncertainties of geotechnical analyses, with a particular focus on cone penetration testing, finite element modelling and slope stability analysis.

Trondheim, 10/06/2020

Hayden Joe

Acknowledgement

I would like to thank my supervisors Jean-Sebastien L'Heureux and Ragnar Moholdt from the Norwegian Geotechnical Institute for their input and guidance in the initial part of the project and provision of the geotechnical data. Thanks to my NTNU supervisor Ana Priscilla Paniagua López for her help and coordinating between NGI and NTNU. I also would like to thank Professor Gudmund Reidar Eiksund from NTNU for his guidance.

Abstract

In January 2019, a shallow marine landslide occurred at Verdal Port, Norway. This slope failure occurred during ongoing construction for port expansion. The initial geotechnical investigations were heavily reliant on CPTU measurements, and misinterpretations of the ground conditions resulted in erroneous slope stability calculations. This paper used a combination of updated CPTU measurements and finite element modelling to perform slope stability back analyses for the Verdal Port landslide. Different CPTU soil behaviour type classification schemes were utilised to produce various soil profiles, that were imported into the software PLAXIS 2D. These finite element models were used to investigate the soil strength parameters, potential failure mechanisms, tidal influences, and geological structure while highlighting the uncertainties associated with CPTU based interpretations and providing an indication of how these uncertainties may influence slope stability calculations.

Contents

List of Figures

List of Tables

Abbreviations and Symbols

CPTU	Cone penetration test with pore pressure measurement
SBT	Soil behaviour type
q_t	Corrected cone resistance
q_c	Cone resistance
f_s	Side friction
SBTn	Normalised soil behaviour type
SBTnm	Modified, normalised behaviour type
γ	Unit weight
R_f	Friction ratio
B_q	Net pore pressure normalised by net cone resistance
F_r	Normalised friction ratio
Q_t	Normalised cone resistance corrected for pore pressure
U_2	Normalised pore pressure
u2	Pore pressure measured behind the cone
Q_{tn}	Updated normalised cone resistance
SCPTU	Seismic cone penetration test
CCS	Clay-like, contractive, sensitive
TC	Transitional, contractive
E	Young's Modulus
E_u	Undrained Young's Modulus
FS	Factor of safety
c	Cohesion
Φ	Friction angle

1. Introduction

1.1 Verdal Port Submarine Landslide

On January 8th, 2019, a shallow submarine landslide occurred at Verdal Port (Figure 1.1), located in the Trondelag county of Norway. At the time of failure, port expansion construction work, which included filling, dredging, new pier construction and relocation of breakwaters was being conducted to facilitate storage and shipping of lime.

The landslide was triggered during the construction of a 4 m high fill and the failure occurred when the planned construction was approximately 2 m high. Judging by post-failure seafloor bathymetry (Figure 1.2), the landslide slip surface developed at an average depth of approximately 3.5 – 4 m, and the volume of displaced soil is approximately 300,000 m^3. In addition, 15 m of the construction road was destroyed by the slope failure. The negative consequences of this landslide included increased expenses, construction delay and requirement of extensive slope stabilisation measures which involved dredging and filling to stabilise and repair the slope before construction of the port expansion could recommence.

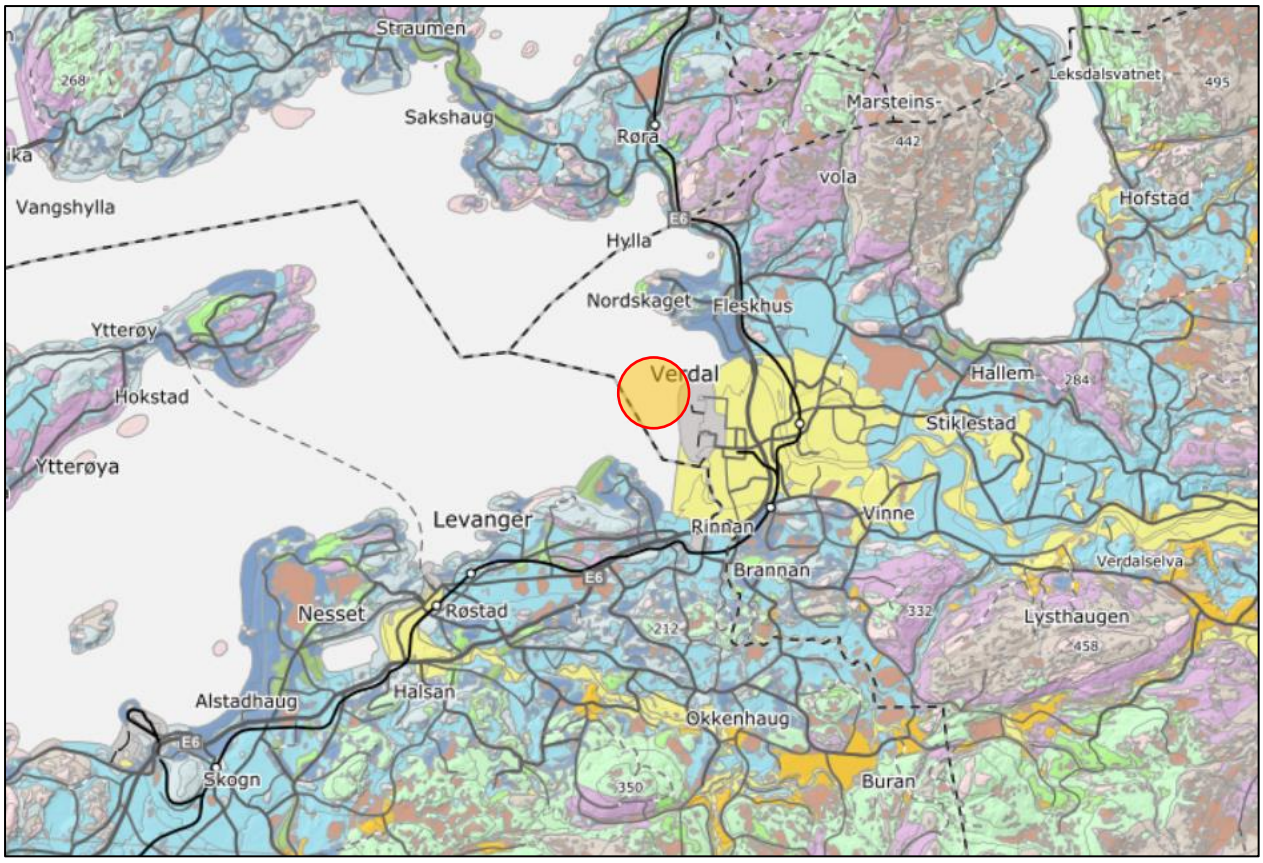

Figure 1.1: Map from NGU showing the location of the submarine landslide at Verdal Port

As the Verdal Port is situated adjacent to the Verdal River Delta the geology is dominated by thick successions of highly variable deltaic sediments which have been suggested by previous geophysical investigations to extend down to 100 – 150 m. Due to this fact, no rock was

encountered during any of the borehole investigations, which descended to a maximum depth of 36 m.

In the initial geotechnical investigation by (Hundal and Øiseth, 2019) it was noted that even with closely spaced borehole soundings the geological stratigraphy was difficult to identify due to the complex, heterogeneous and discontinuous deltaic nature of the sediments being investigated. From the cone penetration testing with pore pressure (CPTU) measurements and total sounding results, the sediments directly influenced by the load of the fill were interpreted to be dominated by silt and sand materials. Because of this interpretation, the original slope stability analysis was conducted using only effective stresses (assuming fully drained conditions), which gave a satisfactory factor of safety with respect to slope stability, even after completion of the 4 m high construction.

The post slide seabed morphology and further geotechnical investigations from (Moholdt, 2019) have indicated that there were thin layers of clay that were unidentified in the original geotechnical investigations. (Moholdt, 2019) has suggested that the unidentified clay played a major role in the landslide development at Verdal Port. It is thought the landslide either initiated within one of these previously unidentified, weak layers of clay or that the clay presence and its associated undrained properties facilitated excess pore pressure generation in adjacent sand sediments, leading to collapse (Moholdt, 2019).

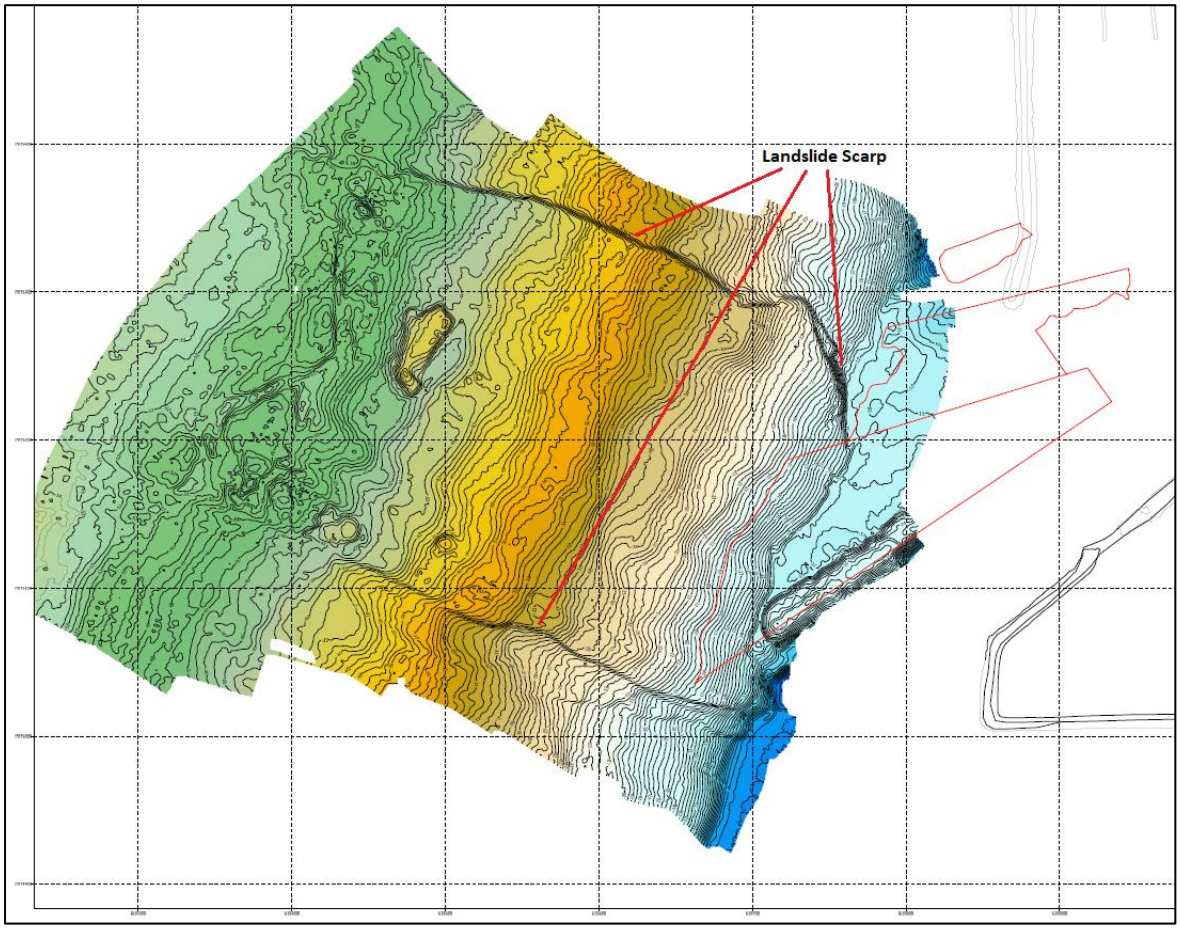

Figure 1.2: Post landslide bathymetry obtained on 12th January 2019, showing the formation of the landslide scarp

The misidentification of this clay was probably a result of the complexity and thin nature of the sediments, which can introduce significant error to CPTU data. Further post-failure geotechnical analyses have indicated that undrained conditions associated with thin clay layers are likely to have an unfavourable influence on the stability and geotechnical behaviour of the slope. It is therefore obvious that undrained slope stability analyses should also have been considered in the original slope stability investigation.

1.2 Geological Background and Event Bed Formation

During the Pleistocene, Trondheim Fjord and much of Norway was subjected to extensive glaciation (Bjerrum, 1955). Repeated glaciations produced glacio-erosional processes that incised bedrock causing extreme steepening of valleys, resulting in the formation of distinct fjord topography that is commonly observed in Western Norway. Norwegian fjords are characterised by extreme topographic variations ranging from high mountains to deep marine basins over relatively short horizontal distances.

Increases in climate temperature resulted in glacial melting, this glacial melt transported soil and rock into marine basins where they accumulated, forming marine clays and other marine sediments (Bjerrum, 1955). The rapid unloading due to deglaciation subsequently produced isostatic rebound, uplifting many of these marine sediments above sea level. These isostatic rebound effects greatly outweighed the rise of sea level due to increased water volume (Bjerrum, 1955). The subsequent changes of the groundwater regime in the uplifted marine clays caused groundwater to flow through the clays, this process leached the marine clays, replacing saltwater in the pores with freshwater (Bjerrum, 1955), which ultimately led to the formation of quick clay. As a result, there is extensive quick clay cover throughout lowlands in the Trondelag region (L'Heureux et al., 2009).

Sedimentary event bed sequences are often deposited in marine environments as a result of hyperpycnal plumes or debris flows that have formed due to extraordinary events such as floods, landslides, earthquakes or rapid snowmelt (Hansen et al., 2011). There have been several large quick clay landslide failures in the Trondheim region that have been well documented (L'Heureux et al., 2009), such as the devastating 1893 Verdal landslide, which remains Norway's most deadly landslide event in with 116 human casualties (Bæverfjord and Thakur, 2008).

The weak layers in Norwegian fjord sediments are often clay-rich layers associated with event bed formations (Hansen et al., 2011). These weak layers are generally softer and more sensitive than surrounding sediments and frequently occur on regional scales throughout Norwegian fjords (L'Heureux et al., 2012). Clay rich layers at the Nidelva river delta have been interpreted by (Hansen et al., 2011) as event bed formations and it is suggested by (L'Heureux et al., 2009) that terrestrial quick clay slides along the Nidelva river are responsible for the increased sediment supply that led to the formation of such event beds.

Due to their unfavourable geotechnical properties, these event beds are commonly linked to submarine slope failures throughout Norwegian fjords. Failure through such event beds typically produces translational landslides, characterised by smooth, planar rupture surfaces with distinct head scarps (L'Heureux et al., 2011).

As the Nidelva river delta is situated in the Trondheim Fjord, around 60 km southwest of the Verdal River Delta, the regional extent of the event beds and proximity of the two deltaic systems suggests that similar geological processes could likely occur at both these locations.

With respect to the slope failure that occurred at Verdal Port, the weak, clay-rich failure bed is hypothesised to have formed by similar event bed depositional processes (Moholdt, 2019). From the local sedimentation rates and this layers locality and depth, a rough estimate by (Moholdt, 2019) has indicated that it is possible this unit was formed as a result of the 1893 Verdal Slide, which would have likely generated favourable conditions for event bed formation.

1.3 Objectives

The main goals of this paper are to:

- Investigate the uncertainties associated with CPTU measurements and identify how these may have contributed to the erroneous slope stability analysis at Verdal Port.
- Apply CPTU processing techniques and investigate different SBT (soil behaviour type) classification methods to account for variability between SBT classification schemes.
- Use updated CPTU data to produce feasible, soil profile scenarios. These soil profiles will be used for finite element modelling in PLAXIS 2D to investigate the most likely soil profile and landslide failure mechanism.
- Perform slope stability back analysis using PLAXIS 2D to estimate the strength properties of the weak clay layer.
- Compare soil characteristics obtained during the investigation to literature, in order to investigate the possibility of weak clay layer being related to event bed deposition.

For the investigation, CPTU data obtained by (Hundal and Øiseth, 2019) was re-processed using methods such as the inverse filtering procedure developed by (Boulanger and DeJong, 2018), with the aim of producing more reliable soil profiles from multiple SBT classification charts developed in (Robertson et al., 1986, Robertson, 1990, Robertson, 2010, Robertson, 2016). The results obtained from the different SBT classification charts were compared to analyse the reliability of each classification system and variability of soil profiles they produced.

The updated soil profiles were then used for finite element slope stability back analysis in PLAXIS 2D, while finite element modelling was used to analyse soil strength parameters, geological structure, conditions influencing failure and the failure mechanism of the Verdal Port submarine landslide.

The geotechnical strength parameters were then compared to geotechnical characteristics of the event bed formations which have been observed in the Trondheim Fjord and other Norwegian fjords in (L'Heureux et al., 2011, L'Heureux et al., 2012, Hansen et al., 2011). This was undertaken to give insight into the possible deposition mechanisms of the thin clay layer and indicate if it is plausible that the formation of this clay layer was associated with terrestrial quick clay slides that had occurred along the Verdal River, such as the well-known Verdal Landslide that occurred in 1893 and was suggested as a possible source by (Moholdt, 2019).

1.4 Relevance

Loss of human life is a serious consequence related to landslide events, especially when a landslide occurs in highly populated areas. Landslide damages can also result in considerable economic loss. (Schuster, 1996) estimated the following losses in USD per year from landslide events:

- USA: $2 billion.
- Japan: $4.5 billion.
- India: $1.5 billion.
- Italy: $ 2.6 billion.

Both landslide frequency and consequence severity are predicted to increase in the future due to a combination of increasing populations, deforestation, development in landslide susceptible areas, urbanisation and climate change favouring more intense rainfall events (Schuster, 1996). Therefore, it is becoming increasingly important to understand the geological, geotechnical and hydrological aspects of slopes so that we can predict, avoid and mitigate landslide events and minimise the detrimental impacts on society and the economy.

Near-shore landslides are more of a threat than offshore landslides as they more often affect coastal areas where human populations and structures are concentrated. Landslides that occur into or within water bodies have the ability to produce secondary effects such as displacement waves and damming of rivers, which can be followed by rapid failure. These secondary effects can have devastating impacts on society and infrastructure such as in (Hermanns et al., 2014) and (L'Heureux et al., 2011).

Populations and infrastructures along coastlines are increasing rapidly and in 2012 it was estimated that around 30% of the global population lives within 60 km of the coastline (Yamada et al., 2012), therefore the consequences of coastal and submarine landslides are growing. In the near future the impacts of climate change are expected to contribute to an increased frequency of landslides due to snowmelt, rising sea levels (Yamada et al., 2012) and increased intensity and duration of rainfall events in many regions (Gariano et al., 2017).

Fjords environments are often targeted for human construction and engineering as they are sheltered and provide excellent locations to build ports. However, due to their extreme topography, the only suitable land to build such structures is often the unstable river deltas (Hampton et al., 1996).

Therefore, just like terrestrial landslides, there is a need to better understand submarine and near-shore landslides in order to develop protect the communities at risk. Soft soil samples of satisfactory quality taken from marine environments are often very difficult or impossible to obtain, therefore, a better understanding of geotechnical investigation tools such as CPTU will allow greater geotechnical understanding and more reliable slope stability assessment in such environments, resulting in the reduced frequency of human-induced slope failures.

2. Inverse filtering for thin layer correction

2.1 Method

Although CPTU may measure the cone resistance (q_t) and side friction (f_s) in thick, homogenous soil layers with sufficient accuracy for use in geotechnical investigation, there are difficulties encountered in the transition zone when the CPTU cone penetrates from one soil layer to another (Ahmadi and Robertson, 2005).

Within this transition zone, there is a gradual change in measured cone resistance due to the fact that measured tip resistance is influenced by the soil above and below the CPTU cone (Treadwell, 1976). The soil within 10 – 30 diameters from the cone tip can have an impact on the recorded measurement, this zone of soil influence is therefore 0.35 – 1.3 m for standard CPTU cones (Boulanger and DeJong, 2018). Due to the extent of vertical soil influence, the transition zone effect can be highly problematic for cone resistance and side friction measurements in thinly layered soils where several distinct soil layers may be present over the length of the influence zone, which in turn will produce unreliable cone resistance values. An illustration of the layer transition effect is shown in figure 2.1.

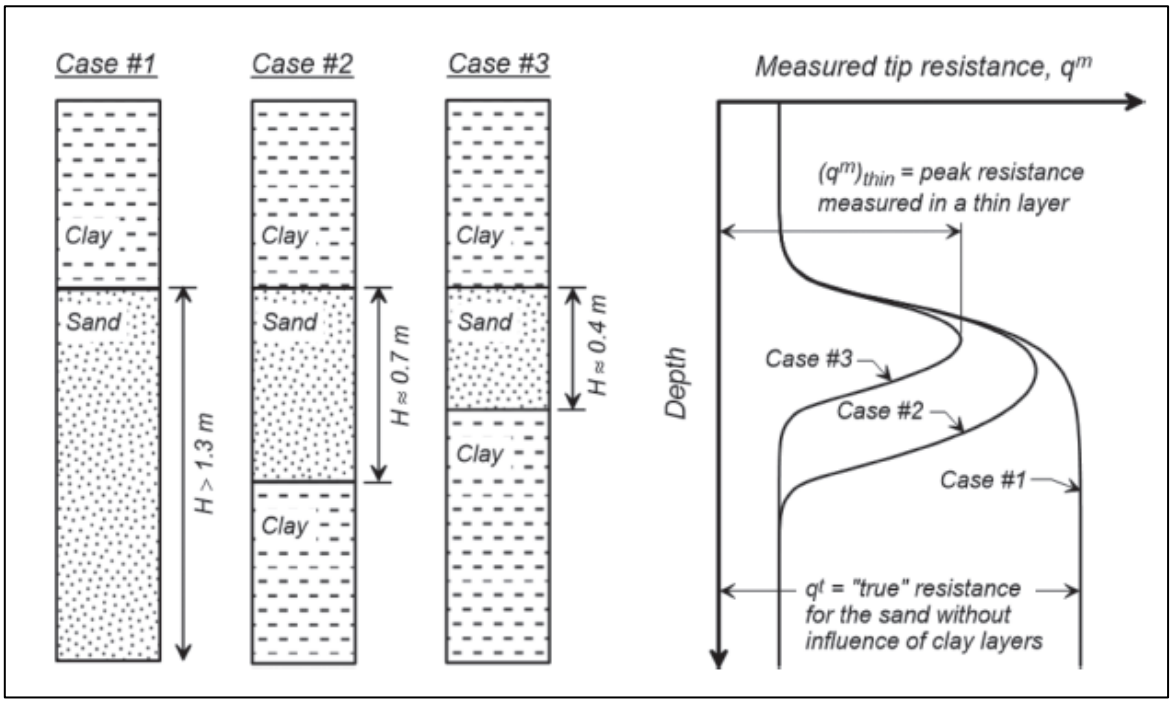

Figure 2.1: Illustration of the transition zone and thin layer effect on CPTU measurements for three different stratigraphic sequences by (Boulanger and DeJong, 2018), modified from (Fear and Robertson, 1995)

(Lunne et al., 1997) has shown that the cone resistance responds much faster in soft soils than stiff soils and the CPTU can identify soft layers down to a thickness of 7.5 – 10 cm, whereas erroneous cone resistance values may be registered in stiff soils that are less than 75 cm thick. Therefore measurements of cone resistance and sleeve friction are dependent on the soil properties and thickness of all soils within the zone of influence, rather than just the soil in which the CPTU is embedded (Boulanger and DeJong, 2018).

The inverse filtering method proposed by (Boulanger and DeJong, 2018) has three components, these are described below:

- Model for how the cone penetrometer acts as a low-pass spatial filter in sampling the true distribution of soil resistance versus depth.

- Solution procedure for iteratively determining an estimate of the true cone penetration resistance profile from the measured profile given the cone penetration filter model.

- Procedure for identifying sharp transition interfaces and correcting data at those interfaces.

The thin layering and transition zone effects, may not matter in some geotechnical investigations, however, there are several situations in which the effects of thin layering and transition zones can have a great impact on the perceived geotechnical behaviour of the soil in question (Boulanger and DeJong, 2018), such as is thought to be the case with the thin clay layer identified at Verdal Port. Thin clay layers can be masked by these effects and this can be highly problematic for geotechnical projects, some important factors are:

- If very low strength, thin clay layers occur within more competent sand or silt layers, because the CPTU data may overestimate the strength of the soil.
- The contrasts in drainage characteristics are important as clay layers may impede drainage, possibly leading to the build-up of excess pore pressure, which will destabilise and possibly liquify sandy materials. This is especially true if loads are applied to the soil.

It is important to minimise the thin layering and transition zone uncertainties at Verdal Port because the complex nature of the thin interbedded deltaic sediments encountered is highly unfavourable with respect to the introduction of error to CPTU measurements. This potential error is a result of the abundance of thin layers with varying geotechnical properties and their associated transition zones. If the errors associated with CPTU measurements are not accounted for it can lead to further errors when the data is used for SBT classification. This is because underestimating or overestimating the strength of soil will likely lead to erroneous SBT zone classification. The SBT classification schemes and their SBT zones are discussed in detail in section 3.

For this investigation, the inverse filtering method proposed by (Boulanger and DeJong, 2018) was applied to the Verdal Port CPTU data using the CPTU interpretation software CPeT-IT from Geologismiki. The objective of applying the inverse filtering method by (Boulanger and DeJong, 2018) was to reduce the thin layering, transition zone and effects on CPTU data in order to minimise the uncertainties and make the processed CPTU measurements more reliable and realistic so that accurate soil profiles could be constructed for use in the finite element analysis.

2.2 Results

The inverse filtering method significantly reduces the thin layering and transition zone effects involved with CPTU measurements, by producing much sharper defined peaks and troughs, as shown in Figure 2.2. Comparisons between the unfiltered and filtered SBT, SBTn and SBTnm profiles show a significant difference in SBT classification throughout the soil profile, especially in sections where very thin layering is observed. However, it is noted that there is little to no change between the unfiltered and filtered SBT classifications with respect to the sensitive, weak clay layer that is situated at an approximate depth of 3.5 – 4 m.

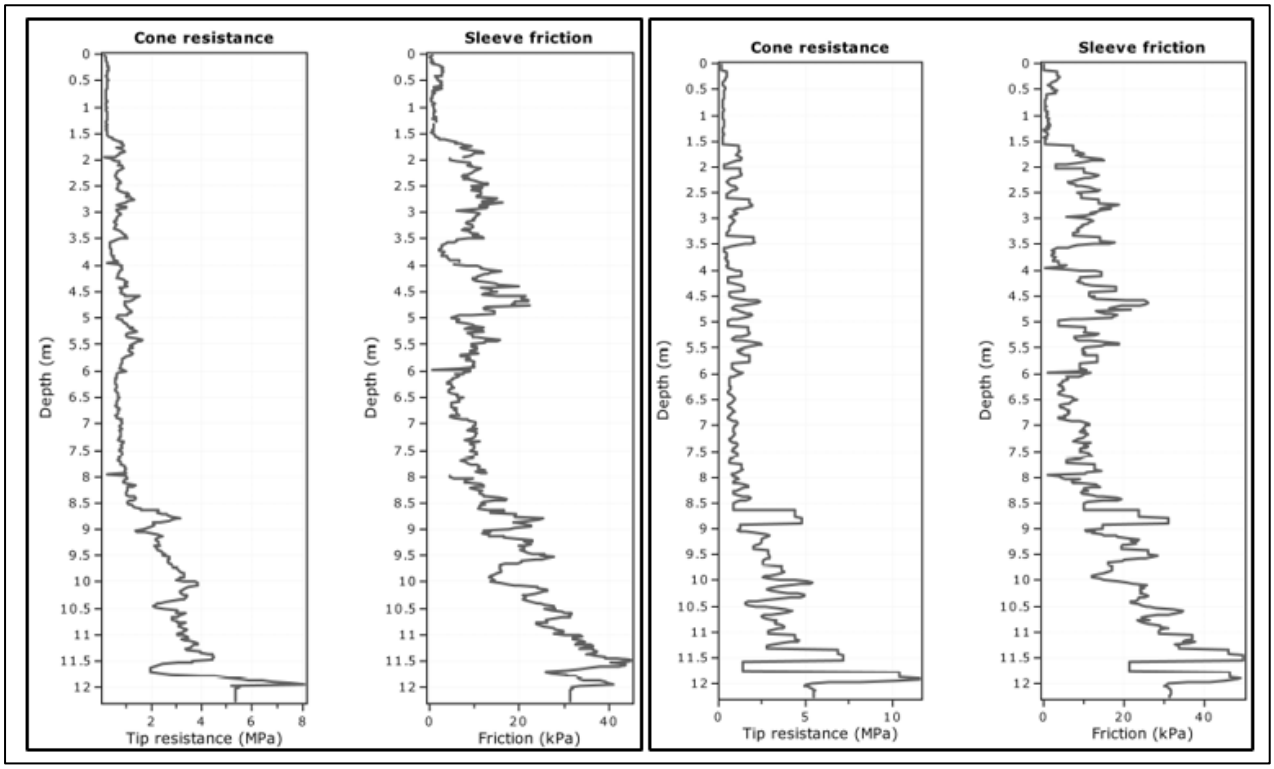

Figure 2.2: Comparison of q_t and f_s from CPTU 1 before (left) and after (right) the inverse filtering method has been applied

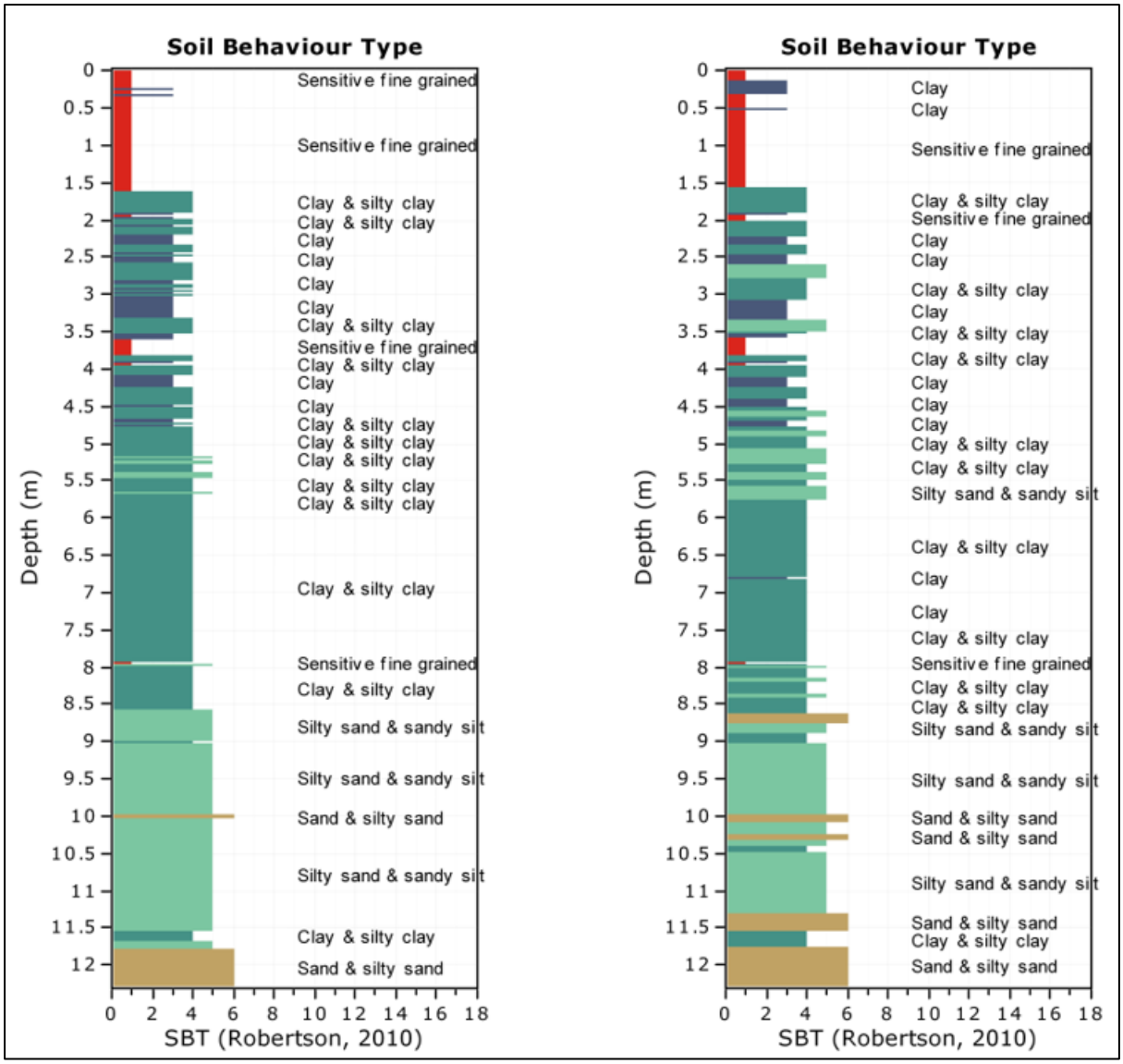

Figure 2.3: Comparison of SBT (Robertson, 2010) soil profiles before (left) and after (right) inverse filter method was applied

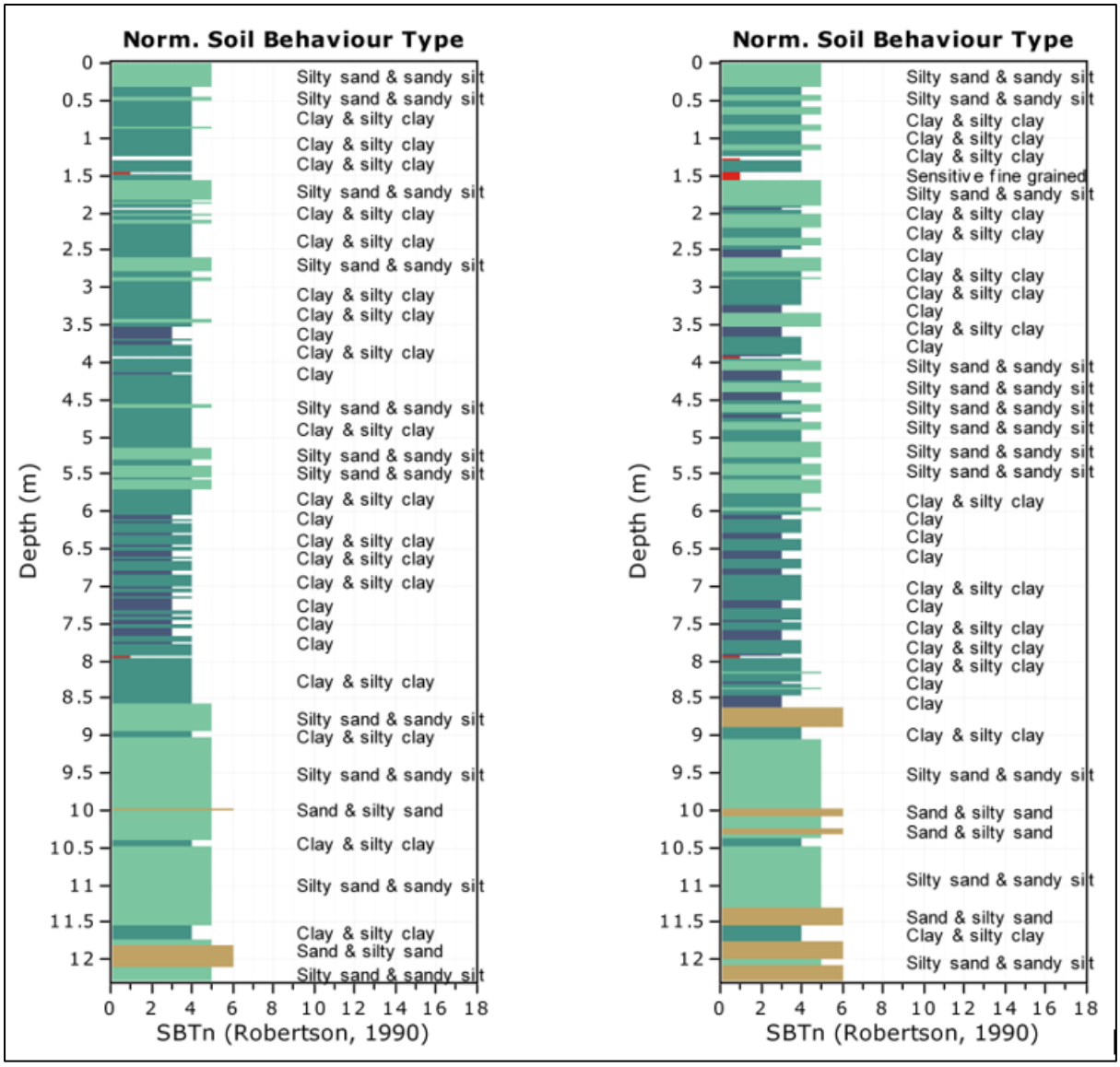

Figure 2.4: Comparison of SBTn (Robertson, 1990) soil profiles before (left) and after (right) inverse filtering was applied

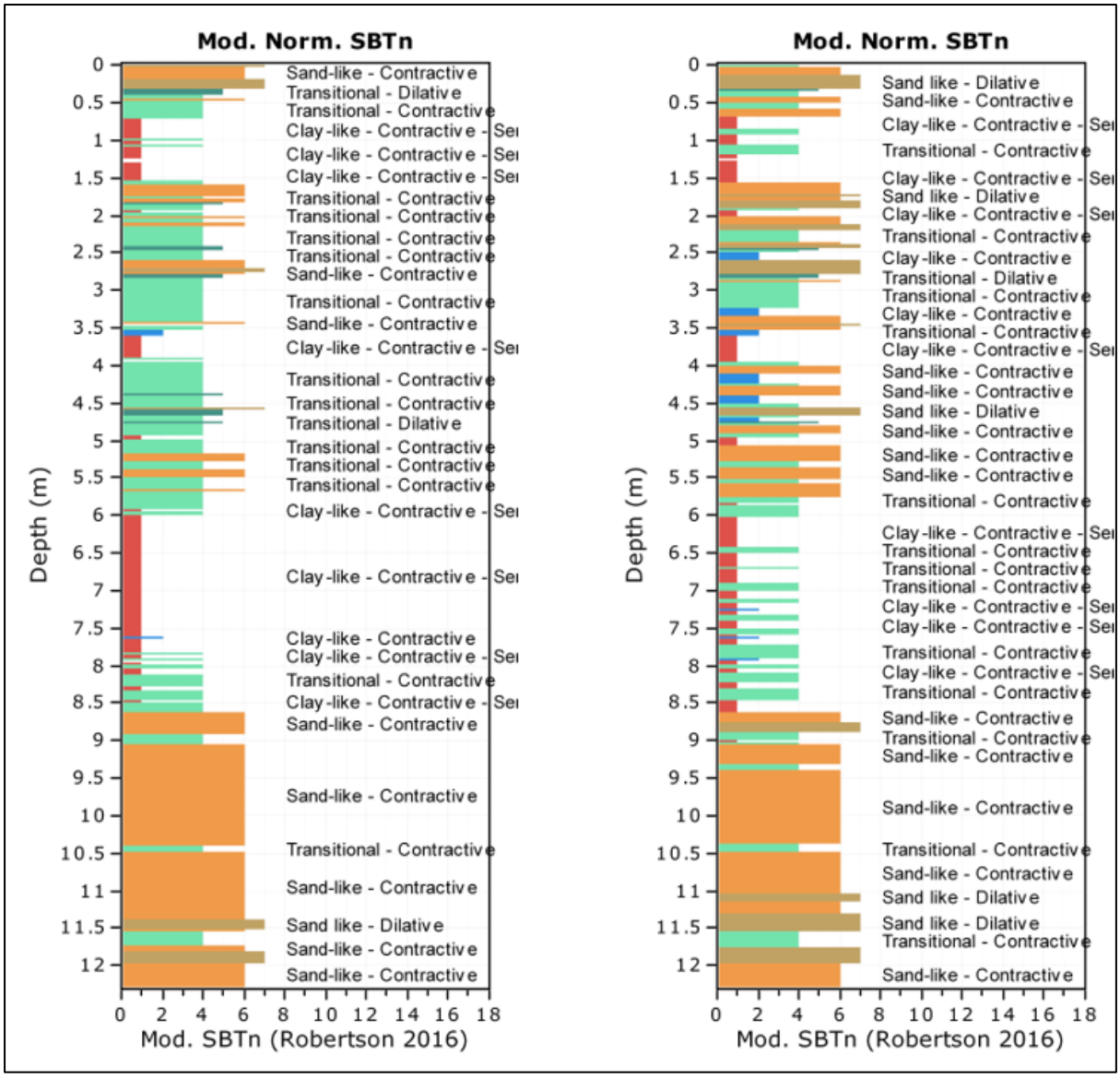

Figure 2.5: Comparison of SBTnm (Robertson, 2016) soil profiles before (left) and after (right) inverse filtering applied

2.3 Discussion

Figure 2.2 shows that individual, thin layers are more clearly defined due to the increase in the resolution which is achieved by minimising the transition zone effect and creating sharper transitions between peaks and troughs of f_s and q_t measurements.

The inverse filtering correction has some influence on the soil profiles generated SBT, SBTn and SBTnm as some soil layers change SBT zone. However, for the SBT and SBTnm profiles, the effects are minimal with respect to the weak clay layer, which is of most importance for the finite element modelling of the Verdal Port slide. These soil profiles are compared in figures 2.3, 2.4 and 2.5 and the lack of difference is probably due to the fact that the cone resistance responds better in thin soft layers than in thin stiff layers. This is because the distance that the CPTU senses increases with stiffness (Lunne et al., 1997). In addition, the SBT zone would only change if the soils were already close to soil zone boundaries, because the inverse filtering effects do not change q_t and f_s values dramatically.

The SBTn unfiltered profile (figure 2.4) shows a gap at a depth of 3.95 – 3.97 m, while the filtered SBTn profile indicates that this gap is occupied by sensitive, fine-grained soil. This gap is due to an anomaly in the CPTU 1 data, which indicates that soil with negative side friction is present at this depth. For modelling purposes, this gap has been assumed to be a sensitive fine-grained soil because side friction provides a rough estimate of the remoulded shear strength of a soil and a negative value indicates that the remoulded shear strength is very low which would result in high sensitivity. However, it may be that this measurement is due to a systematic error that occurred during the CPTU penetration and should be treated with caution.

3. Robertson's SBT Classification

3.1 Method

(Douglas and Olsen, 1981) determined that CPTU classification charts poorly predict soil type based on grain size distribution. However, these charts can be extremely useful as to understanding the behaviour of the soil, as these charts give an insight into several soil behaviour factors including sensitivity, in-situ stress conditions, over consolidation ratio, void ratio and stiffness (Robertson, 1990).

Studies from (Aas et al., 1988) and (Gillespied, 1989) have found that tip resistance measurements are generally more reliable than sleeve friction measurements, even after corrections accounting for pore pressure influence have been applied. Even though a lower accuracy is observed for sleeve friction measurements, experience indicates that cone resistance, sleeve friction and pore pressure measurements should all be used together to obtain the most reliable CPTU soil classification (Robertson, 1990).

The soil profiles for the landslide stability back analysis were constructed using the inverse filtered CPTU measurements from CPTU 1 and CPTU 2 which define cross-section A-A from (Hundal and Øiseth, 2019) shown in figure 3.1. The stratigraphy of the soils was defined using various CPTU SBT charts which define SBT zones based on tip resistance, side friction and pore pressure measurements. In these charts, soils in zones 1 – 4 are generally assumed to experience undrained conditions, 6 and 7 drained and 5, 8 and 9 partially drained (Robertson, 1990). If a particular soil is classified in different zones for different charts, geotechnical judgment is required. In such cases, the pore pressure dissipation rate is an important factor to consider (Robertson, 1990).

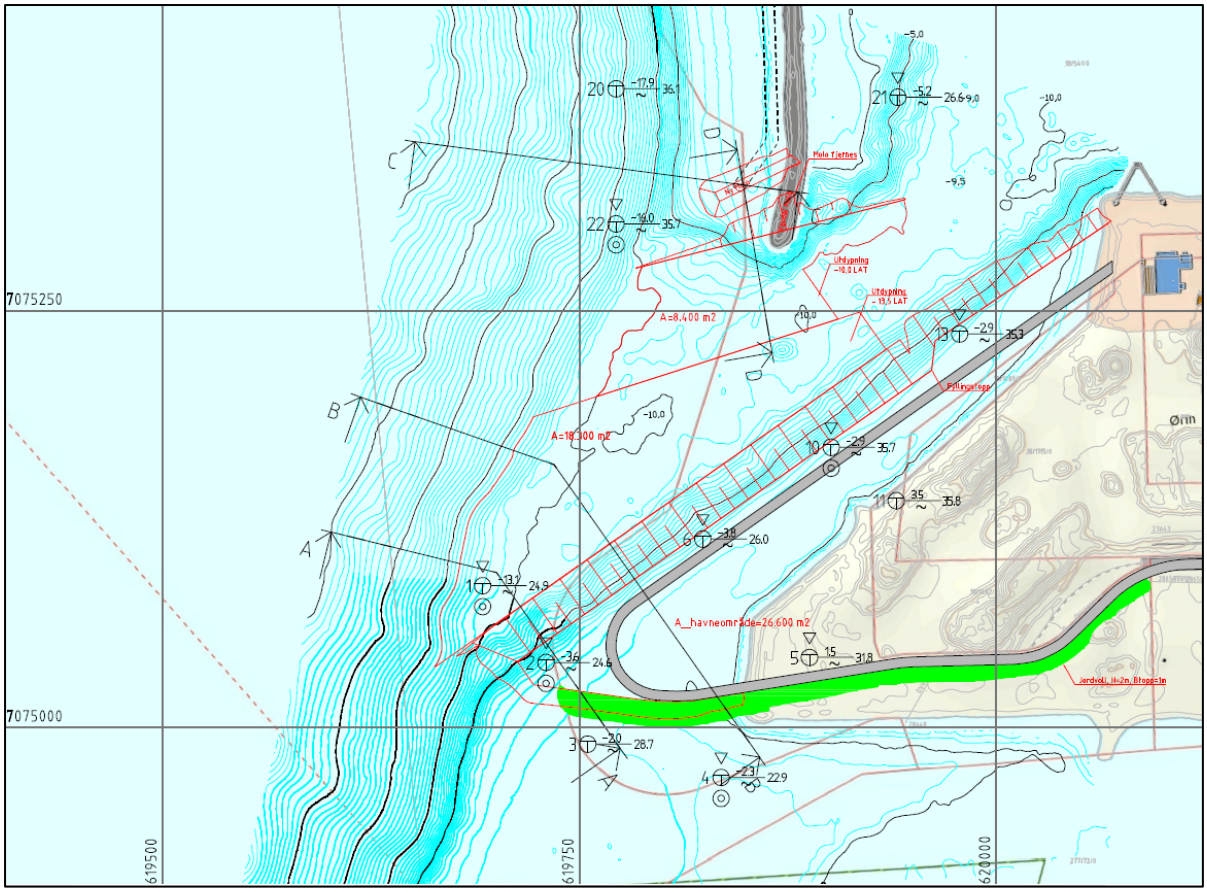

Figure 3.1: Plan view of Verdal Port and borehole locations from (Hundal and Øiseth, 2019)

Three different versions of soil behaviour type classification were used to get an idea of how the different methods influence the final soil profile. The classification schemes used included:

- Soil behaviour type classification (SBT) developed by (Robertson et al., 1986) which was updated and modified in (Robertson, 2010)
- Normalised soil behaviour type (SBTn) which was developed by (Robertson, 1990)
- Modified normalised soil behaviour type classification (SBTnm) which was updated from (Robertson, 1990) in (Robertson, 2016)

The advantages of the (Robertson et al., 1986) and (Robertson, 2010) SBT classification scheme is that is very easy to use and requires only the basic CPTU parameters (Robertson, 2010).

(Robertson et al., 1986) SBT classification charts present q_t/q_c on a log scale and the friction ratio (R_f) on a natural scale, however (Robertson, 2010) proposes an update to the non-normalised SBT classification where a dimensionless cone resistance is presented on the SBT charts as (q_c/pa) where pa is atmospheric pressure (100 kPa) and both R_f and q_c/pa are presented on log scales, this expands the area where R_f is below one percent, increasing the accuracy in this zone (Robertson, 2010). The (Robertson, 2010) update also reduces the number of SBT classification groups to 9 with the goal of simplifying the process of making comparisons

between the SBT and SBTn classification systems. We have therefore used the (Robertson, 2010) SBT classification, as the updated version allows better comparison with the SBTn and SBTnm classification schemes. A table showing the updated SBT zones is presented in Table 3.1.

CPTU soil classification charts that use cone resistance, sleeve friction and pore pressure can have significant error if the CPTU profile penetrates deeper than 30 m (Robertson et al., 1986), as all these factors generally increase with depth and increasing stress conditions (Robertson, 1990). (Wroth, 1984) and (Houlsbyg, 1988) normalised CPTU measurements using the parameters Q_t, B_q and F_r. These normalised methods now have extensive CPTU databases from which SBTn charts were developed in (Robertson, 1990).

The SBTn and SBTnm classification schemes are considered more reliable than SBT because the CPTU parameters are normalised with respect to effective stress to account for the error due to increasing overburden stress with increasing depth (Robertson, 2010). However, normalisation of the CPTU data requires a knowledge of the soil's unit weight and the groundwater regime (Robertson, 2010). If the in-situ vertical effective stress is within the range of 50 – 150 kPa there is generally a minimal difference between the normalised and non-normalised soil behaviour classification systems (Robertson, 2010). The differences between SBTn and SBTnm are discussed in detail in chapter 4.

For the Verdal Port, the heterogeneous and complex soil stratigraphy indicates that the unit weight of the soil varies significantly depending on the layer observed. Laboratory tests conducted by (Ramboll) on samples from boreholes 1, 2, 4 and 10 indicate that the unit weight in Verdal Port sediments varies from 17.6 kN/m^3 to 19.8 kN/m^3. Considering the unit weight variability and that the CPTU penetration depth for both CPTU 1 and CPTU 2 is well below 30 m, the basic SBT classification may give reliable results for some sections of the soil profile. However, there are likely to be significant differences between the SBT and SBTn/SBTnm profiles with respect to the weak clay layer, as the in-situ vertical effective stresses within the weak clay layer are often outside the 50 – 150 kPa range, which could lead to a higher degree of inaccuracy (Robertson, 2010).

SBT zone (Robertson et al., 1986)	SBTn zone (Robertson, 1990)	Proposed common SBT description
1	1	Sensitive fine-grained
2	2	Clay – organic soil
3	3	Clays: clay to silty clay
4 & 5	4	Silt mixtures: clayey silt and silty clay
6 & 7	5	Sand mixtures: silty sand to sandy silt
8	6	Sands: clean sands to silty sands
9 & 10	7	Dense sand to gravelly sand
12	8	Stiff sand to clayey sand*
11	9	Stiff fine-grained*

Table 3.1: (Robertson, 2010) update shows the unification of 12 SBT zones in (Robertson et al., 1986) to 9 SBTn zones in (Robertson, 1990). *Overconsolidated

3.2 Results

The SBTn (Robertson, 1990) B_q chart was used to define the soil profile at CPTU 1 by (Moholdt, 2019), this SBTn interpretation is displayed in figure 3.2. The B_q SBTn classification indicated that there are significant clay layers throughout the soil profile at CPTU 1, while there is an absence of soils classified as sensitive, fine-grained. The B_q chart profiles indicated much thicker clay beds while the CPeT-IT profiles suggested a much higher degree of interbedded clay and silty clay at the same depth.

At CPTU 1 the SBT R_f (friction ratio) chart indicated significant quantities of soils classified as sensitive, fine-grained, while the SBT B_q charts indicated that there is very little sensitive, fine-grained soil. The overall SBT (Robertson, 2010) classification produced in CPeT-IT took the results from both the R_f and B_q charts into account and the interpreted soil profiles are displayed in Figure 3.3. This showed a 24 cm thick sensitive clay layer at depth 3.59 – 3.83 m at CPTU 1. This sensitive clay layer was present at depth 4.83 – 4.85 m at CPTU 2, indicating that the sensitive clay layer gets thinner towards CPTU 2. The SBT zones defined from (Robertson, 2010) classification charts shown in figures 3.4 and 3.5.

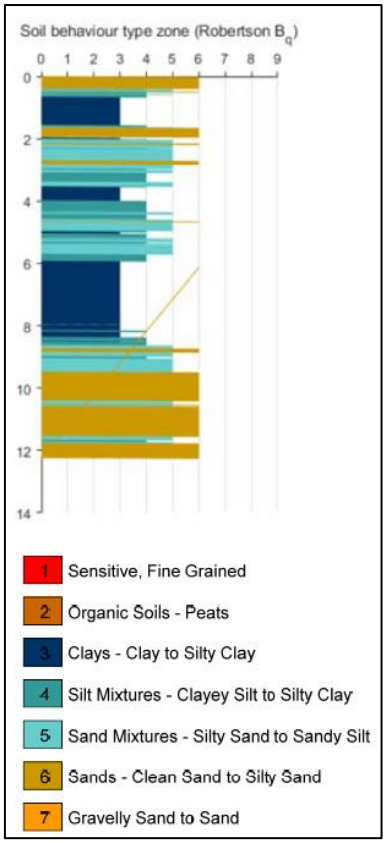

Figure 3.2: CPTU 1 soil profile interpretation from (Moholdt, 2019) based on SBTn (Robertson, 1990)

At CPTU 1 the SBTn - F_r (normalised friction ratio) chart indicated more sensitive fine-grained soil than the SBTn B_q chart, as shown in Figure 3.7. The SBTn (Robertson, 1990) classification interpretations, which combined both the F_r and B_q charts are given in figure 3.6. These identified a 2 cm thick sensitive clay layer at depth 3.95 – 3.97 m at CPTU 1. Therefore, the thickness of sensitive fine-grained soil is reduced in the SBTn soil profile compared to the SBT soil profile.

The sensitive clay layer was not present at CPTU 2, suggesting that the clay layer pinches out somewhere in between CPTU 1 and CPTU 2. The soil behaviour type zones are defined from (Robertson, 1990) classification charts shown in figures 3.7 and 3.8. As previously noted, the CPTU data from 3.95 – 3.97 m had anomalous negative side friction values, which may indicate an error. The possibility of error and the thin nature of this bed indicate that there is a high degree of uncertainty associated with this layer.

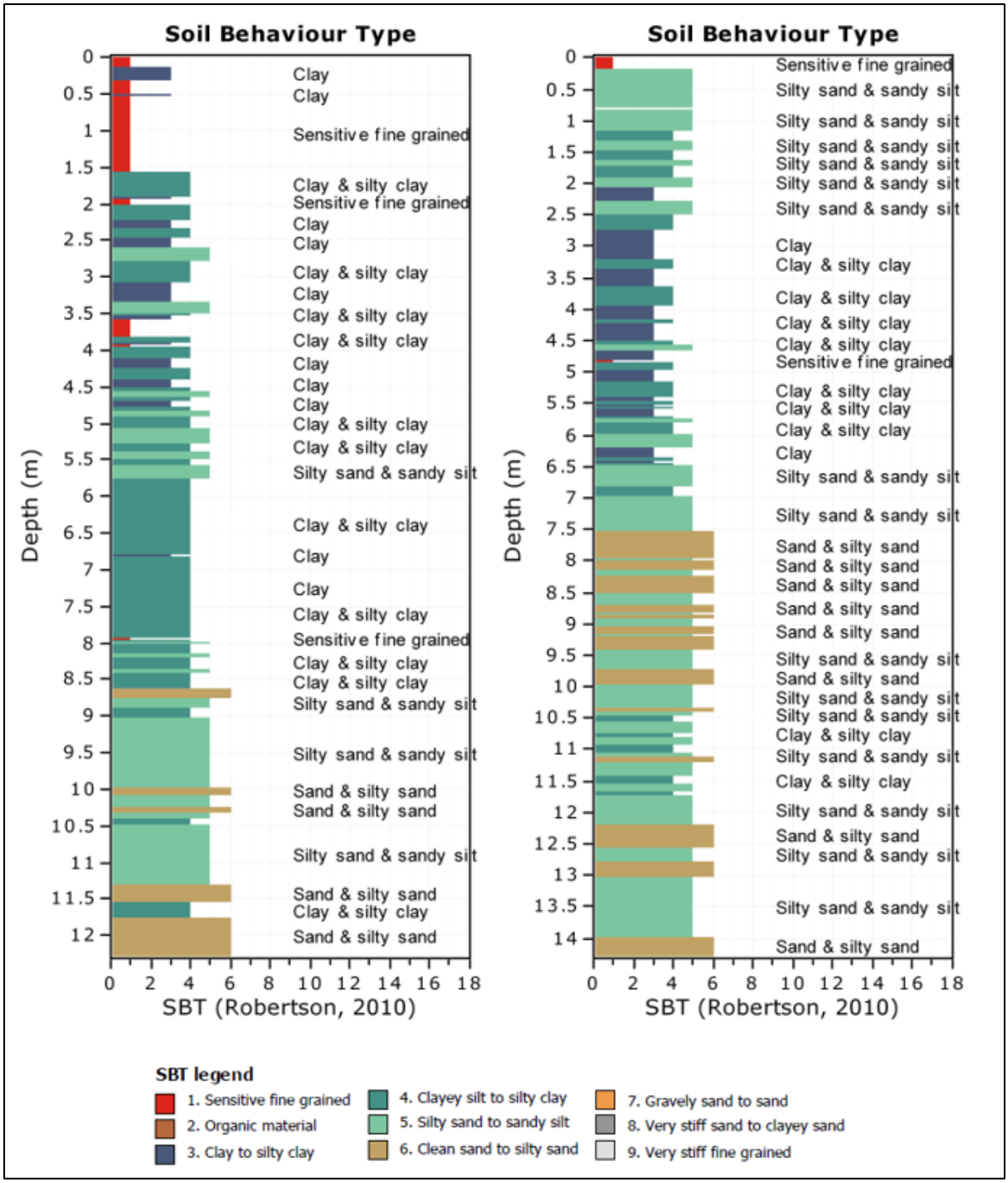

Figure 3.3: Soil profiles generated from CPTU 1 (left) and CPTU 2 (right) measurements using SBT classification (Robertson, 2010)

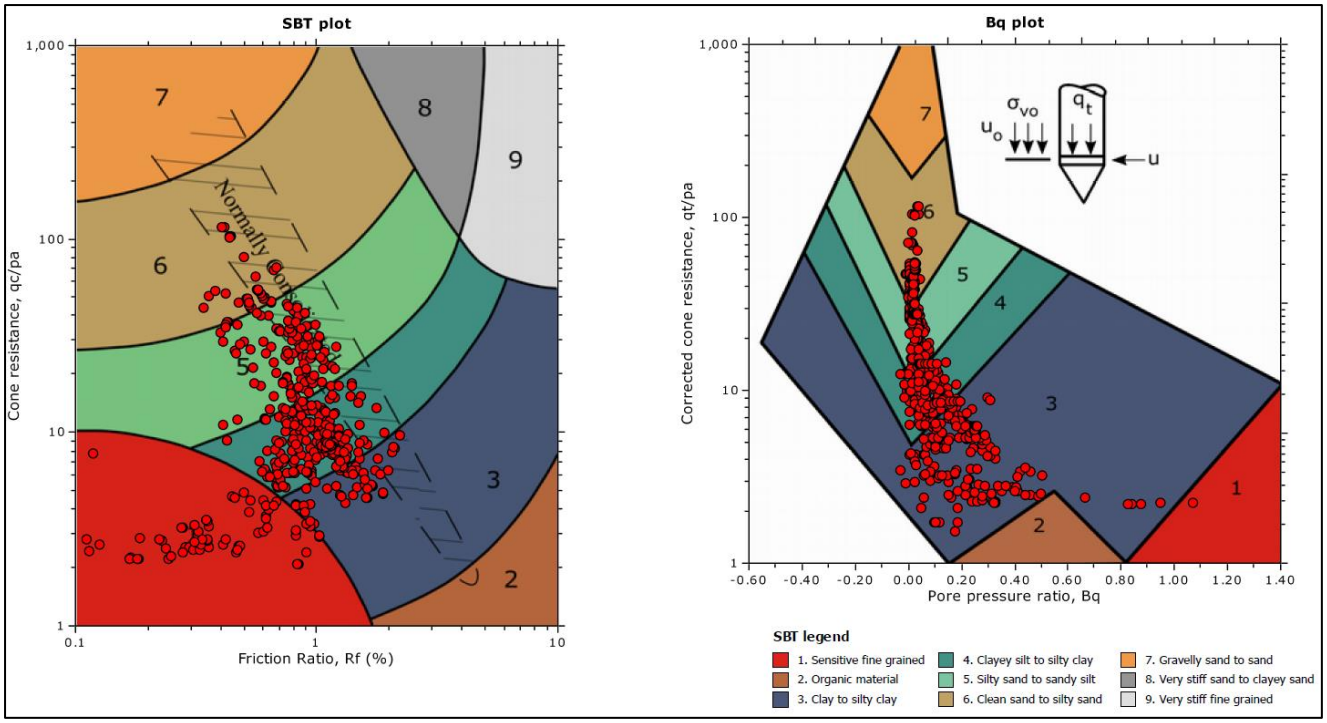

Figure 3.4: SBT and B_q plots for SBT (Robertson, 2010) from CPTU 1

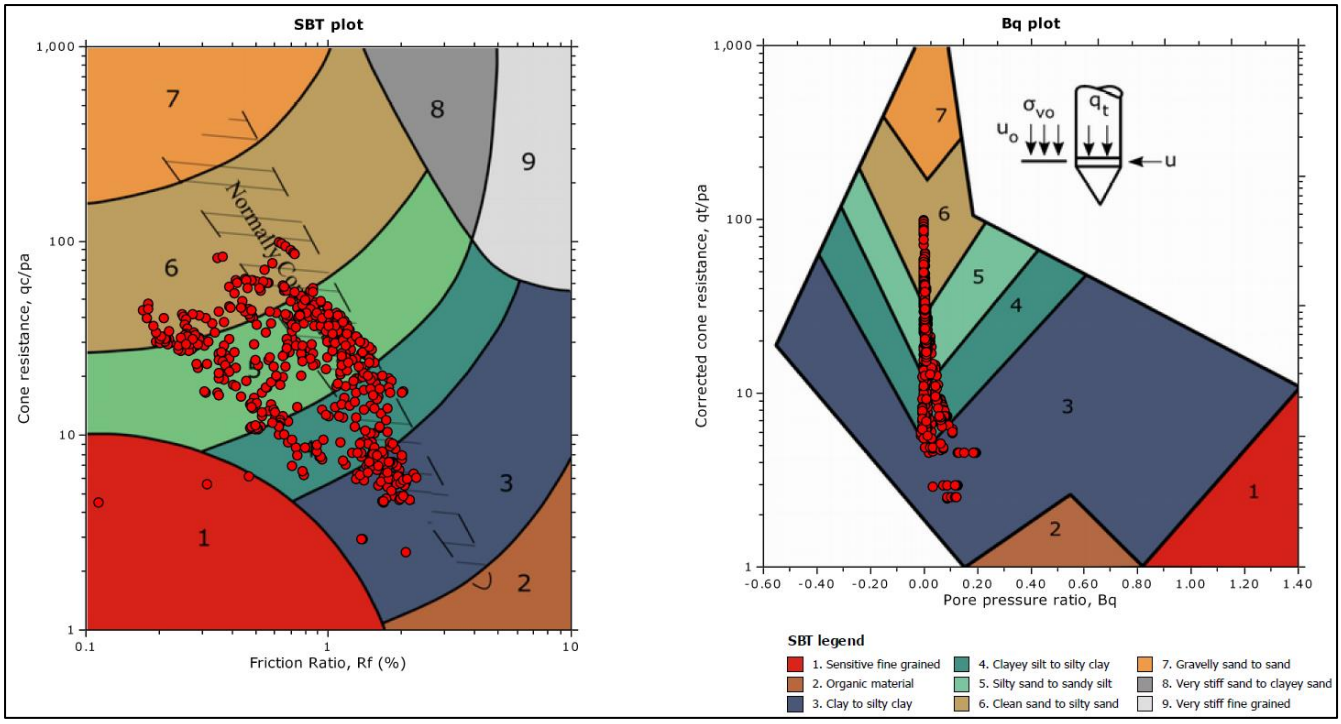

Figure 3.5: SBT and B_q plots for SBT (Robertson, 2010) from CPTU 2

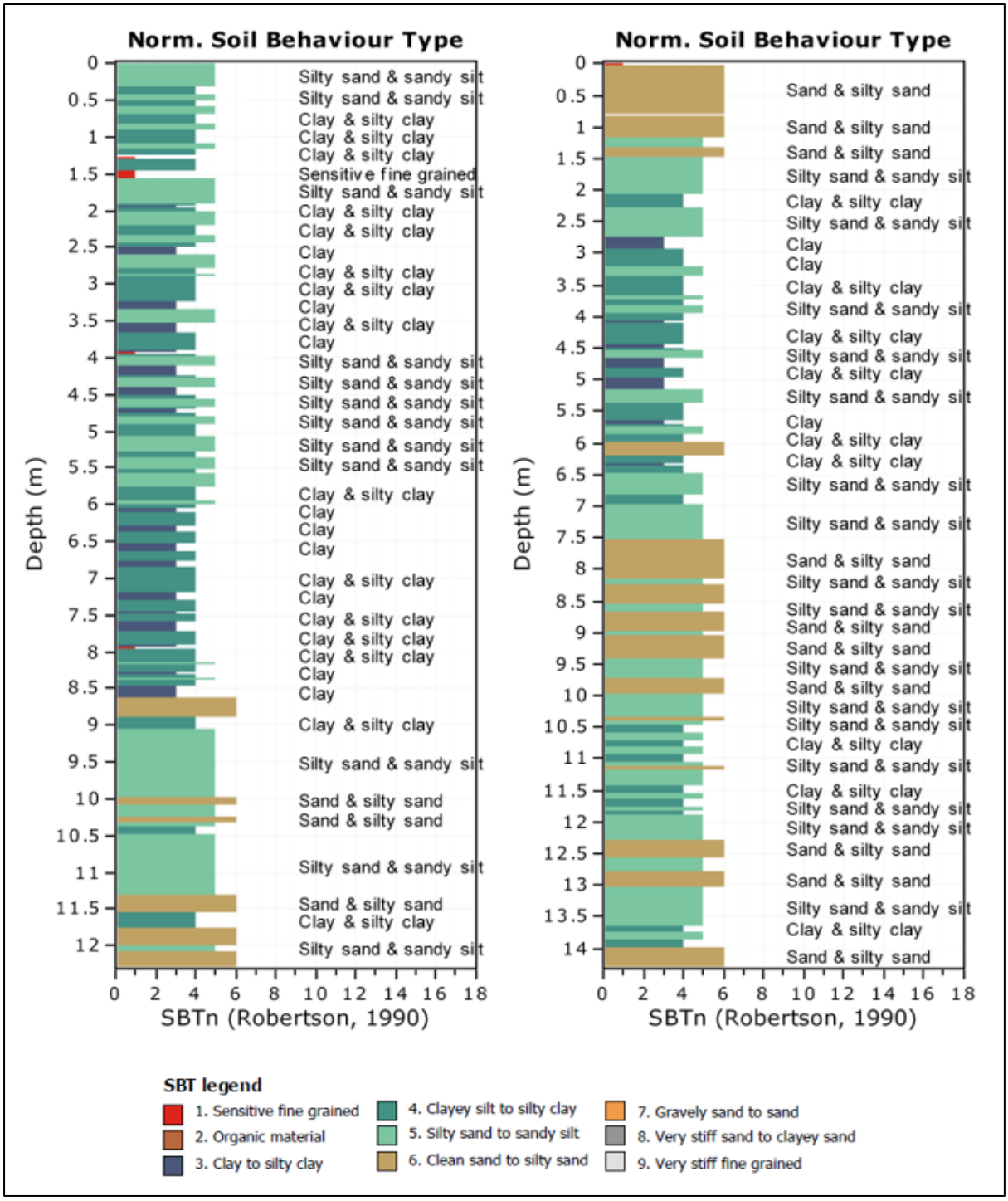

Figure 3.6: Soil profiles generated from CPTU 1 (left) and CPTU 2 (right) measurements using SBTn classification (Robertson, 2010)

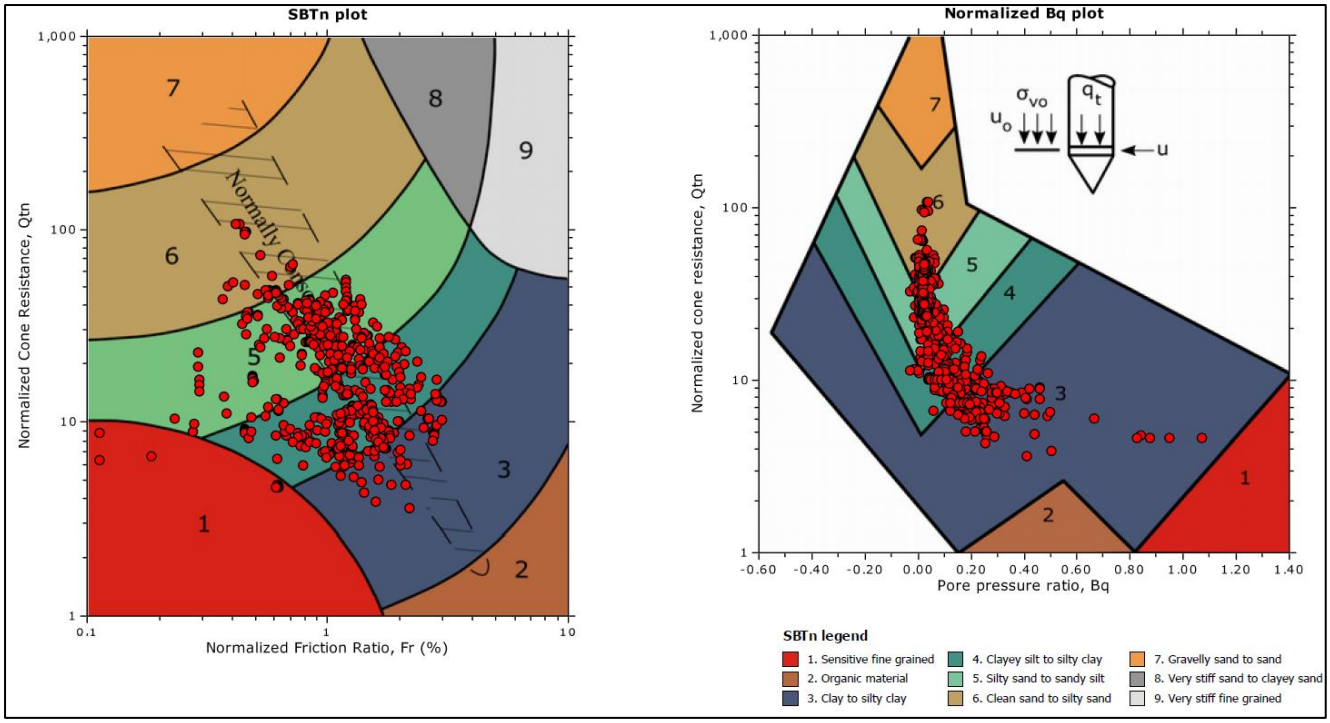

Figure 3.7: SBT and B_q plots for SBTn (Robertson, 1990) from CPTU 1

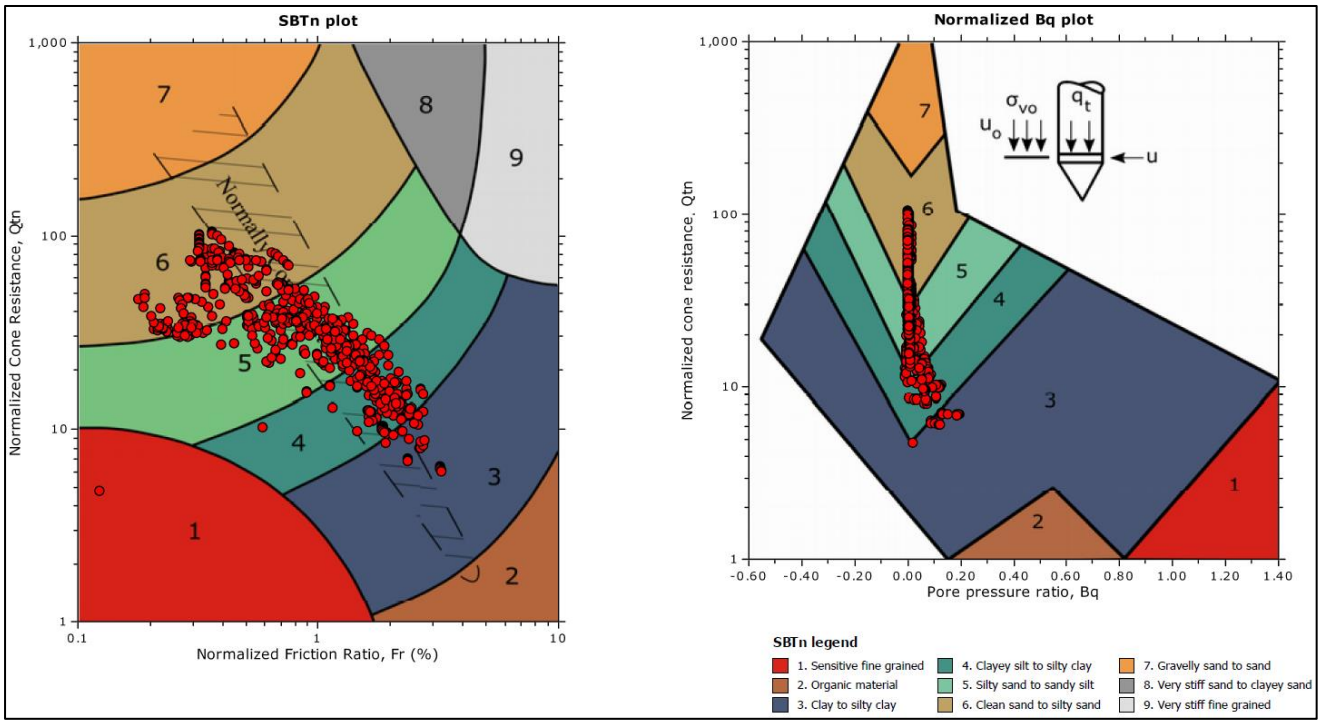

Figure 3.8: SBT and B_q plots for SBTn (Robertson, 1990) from CPTU 2

The SBTnm (Robertson, 2016) classification results are given in figure 3.9. This shows a 38 cm thick sensitive, contractive clay layer at depth 3.59 – 3.97 m at CPTU 1. This sensitive clay layer is not present at CPTU 2, suggesting that the clay layer pinches out somewhere in between CPTU 1 and CPTU 2. The soil behaviour type zones are defined from the (Robertson, 2016) classification charts shown in figure 3.10 and 3.11. The differences between the SBTn and SBTnm classification schemes are discussed in detail in chapter 4.

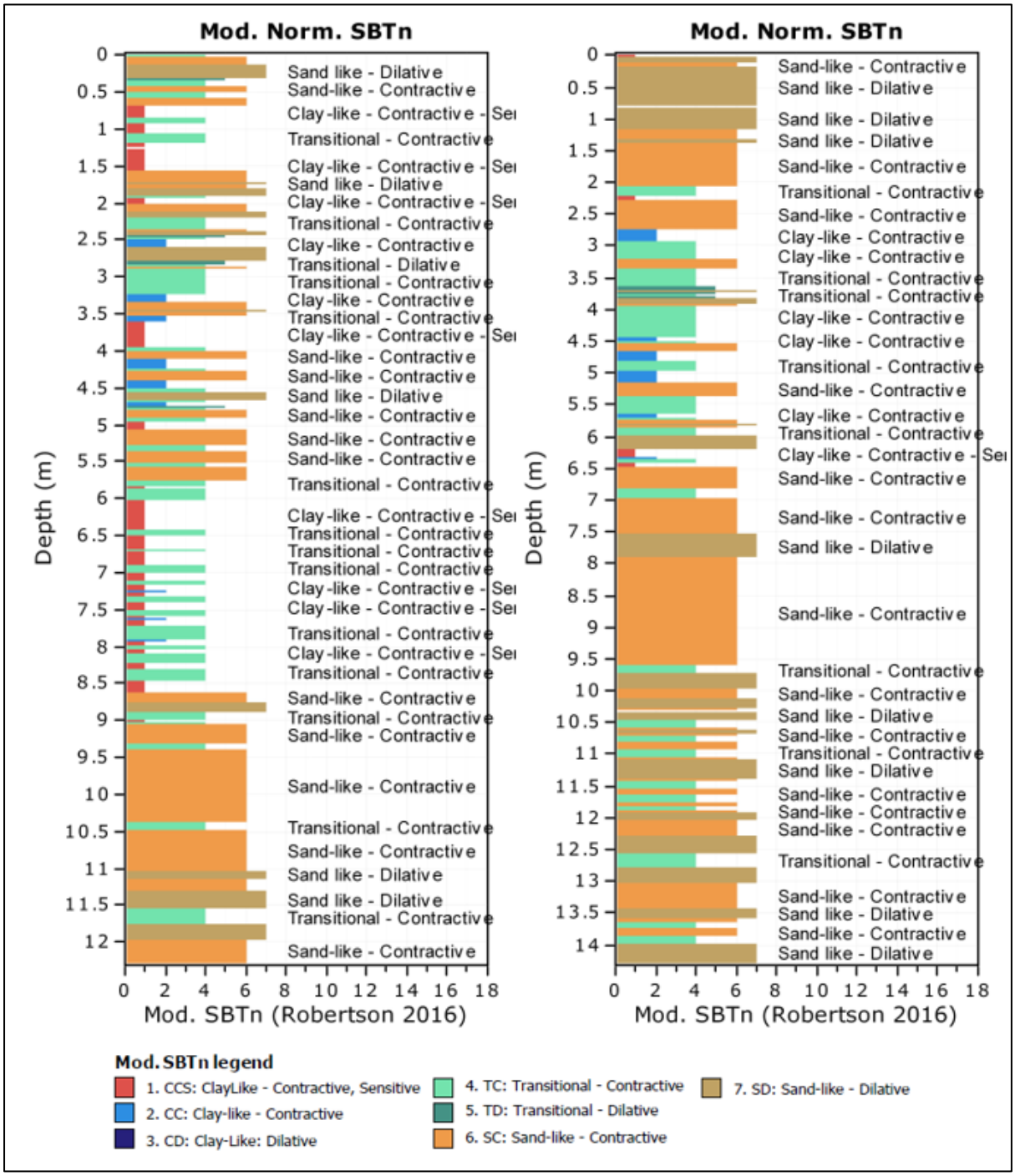

Figure 3.9: Soil profiles generated from CPTU 1 (Left) and CPTU 2 (Right) measurements using SBTnm classification (Robertson, 2016)

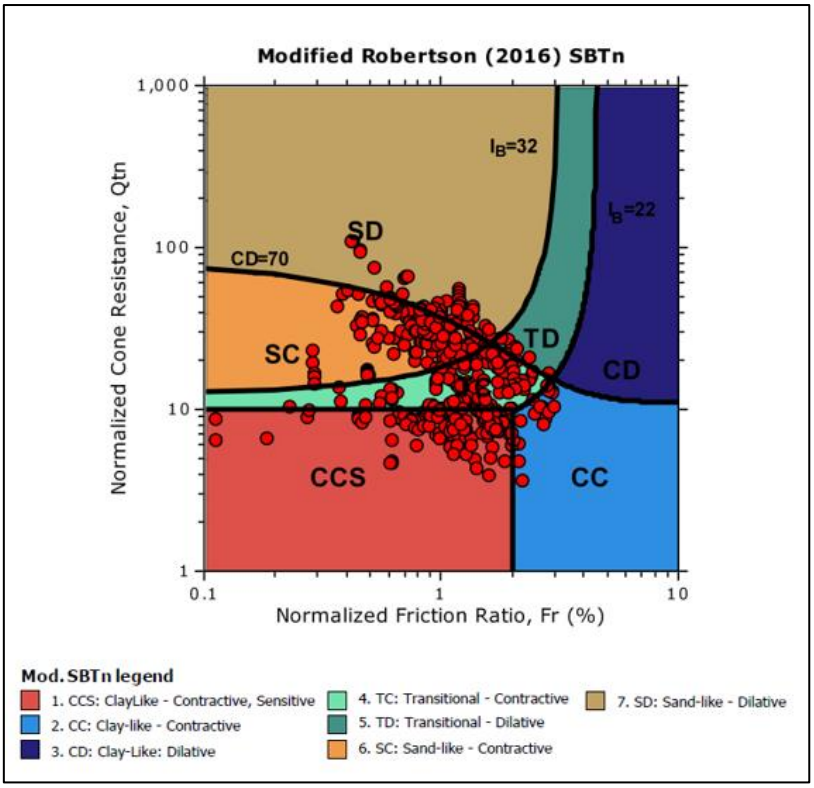

Figure 3.10: SBTnm soil behaviour type zones charts (Robertson, 2016) from CPTU 1

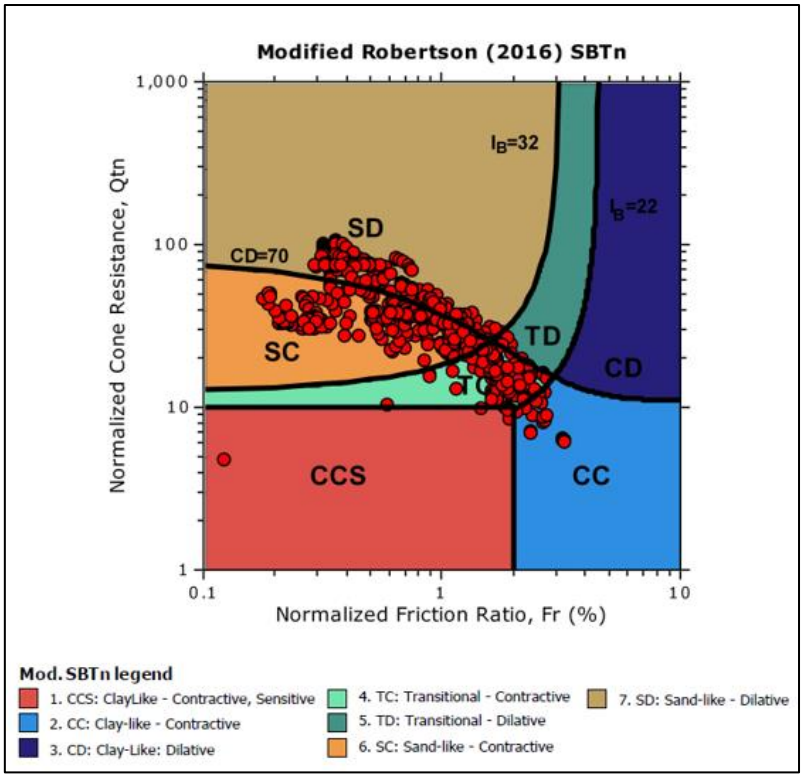

Figure 3.11: SBTnm soil behaviour type zones charts (Robertson, 2016) from CPTU 2

3.3 Discussion

The interpreted soil profile produced in (Moholdt, 2019), using the SBTn B_q chart identifies significant clay layers present at CPTU 1. However, this SBTn interpretation did not indicate the presence of any sensitive fine-grained soils. The differences between the soil profile produced in (Moholdt, 2019) and the soil profiles produced in this investigation is due to the fact that the (Moholdt, 2019) SBTn interpretation used CPTU data that had not had the inverse filtering thin layer correction applied and only uses the (Robertson, 1990) B_q chart.

However, experience indicates that cone resistance, sleeve friction and pore pressure measurements should all be used together to obtain the most reliable CPTU SBT classification (Robertson, 1990). Hence, interpretations made in this investigation that had the inverse filter applied and use the CPeT-IT software to produce SBT interpretations which take into account cone resistance, sleeve friction and pore pressure using the SBT, SBTn and SBTnm charts from (Robertson, 2010), (Robertson, 1990) and (Robertson, 2016) have been considered to be more reliable, and therefore were used for further investigation.

The soil profiles generated from the SBT, SBTn and SBTnm CPTU classification schemes are all significantly different from each other. Of particular importance are the variations observed with respect to the thickness and lateral extent of the weak clay layer. The inferred geometry of the thin clay layer is summarised below in table 3.2. Although the SBTn and SBTnm schemes were expected to produce the most reliable results, soil profiles produced by all three of the SBT classification schemes were used for finite element modelling with PLAXIS 2D to investigate the impact that these differences had on the slope stability analysis at Verdal Port. This was performed to give an insight into the degree of uncertainty that arises when using CPTU measurements and SBT based soil profiles for slope stability investigations.

Classification Scheme	Location	Depth to Sensitive Clay Layer (m)	Thickness of Sensitive Clay (cm)
SBT (Robertson, 2010)	CPTU 1	3.59	24
	CPTU 2	4.83	2
SBTn (Robertson, 1990)	CPTU 1	3.95	2
	CPTU 2	Not Present	0
SBTnM (Robertson, 2016)	CPTU 1	3.59	38
	CPTU 2	Not Present	0

Table 3.2: Resulting weak clay layer morphology indicated by SBT, SBTn and SBTnm

4. SBTn vs SBTnm

4.1 Method

The (Robertson, 1990) SBTn classification has been widely used for over 25 years with great success for ideal soils, which have little to no microstructure, and therefore the effects of microstructure are negligible (Robertson, 2016). However, the SBTn (Robertson, 1990) scheme is not as reliable when used to classify soils which have significant microstructures (Robertson, 2016). The main objective of the modifications of the (Robertson, 1990) SBTn classification scheme, which produced the SBTnm (Robertson, 2016) classification charts, was to identify and account for microstructure within the soils and identify whether a soil displays contractive or dilative behaviour when large strains are introduced (Robertson, 2016). According to (Sergeyev et al., 1980) microstructures are one of the most important factors in determining the properties of clays, as microstructures can have a significant influence on the strength and stiffness of a soil (Robertson, 2016).

Saturated soils that display contractive behaviour when subject to high magnitudes of strain tend to have lower shear strength in undrained loading relative to drained loading (Robertson, 2016). In contrast, saturated, dilative soils tend to have undrained shear strengths that are equal to or greater than the shear strength in drained conditions (Robertson, 2016). Some saturated soils which display contractive behaviour also exhibit strain-softening behaviour when subject to shear in undrained conditions. This loss of strength due to strain-softening can result in flow liquefaction induced failures (Robertson, 2016). For these reasons, it is important to understand the soils dilative or contractive characteristics to better understand the geotechnical behaviour of soil (Robertson, 2016).

Another difference between the SBTnm and SBTn classifications is that the (Robertson, 1990) SBTn classification includes a Q_t-B_q chart, however, (Schneider et al., 2008) found that U_2 is a more reliable measure of normalised pore pressure than B_q. U_2 is given as $\Delta u2/\sigma'$. U_2 is based on u2 which measures pore pressure just behind the tip of the CPTU cone. Where the soil is being sheared at large strain, u2 and therefore U_2 give an indication into how soil responds at high strains (Robertson, 2016). (Robertson, 2016) suggested that positive U_2 values indicate contractive behaviour at high strains, while negative U_2 values indicate dilative behaviour at high strains. As a result of their findings (Schneider et al., 2008) proposed a more reliable Q_t – U_2 chart for soil classification, which was adopted and updated for use in the (Robertson, 2016) SBTnm classification.

The updated Q_t – U_2 chart has been used to classify the weak clay layer observed at Verdal Port based on CPTU measurements, the results are displayed in figure 4.1. The updated Q_{tn} – U2 chart can be used to identify if a soil behaves as an ideal soil or as a soil with microstructure as increasing Q_t and U_2 are indicative of increasing microstructure (Robertson, 2016). The Q_{tn} – F_r chart from (Robertson, 1990) has also been updated in (Robertson, 2016) to add boundaries indicating the contractive or dilative behaviour of the soil. The weak clay encountered at Verdal Port is plotted on this chart in figure 4.2. To make the most reliable assessment, the charts in figures 4.1, and 4.2 should be utilised together with figure 4.3 (Robertson, 2016) which is explained in the following section. It should be noted that seismic cone penetration testing (SCPTU) is required to give the best indication to a soil's microstructural properties. However, no such field investigations were conducted during the Verdal Port geotechnical investigation.

4.2 Results

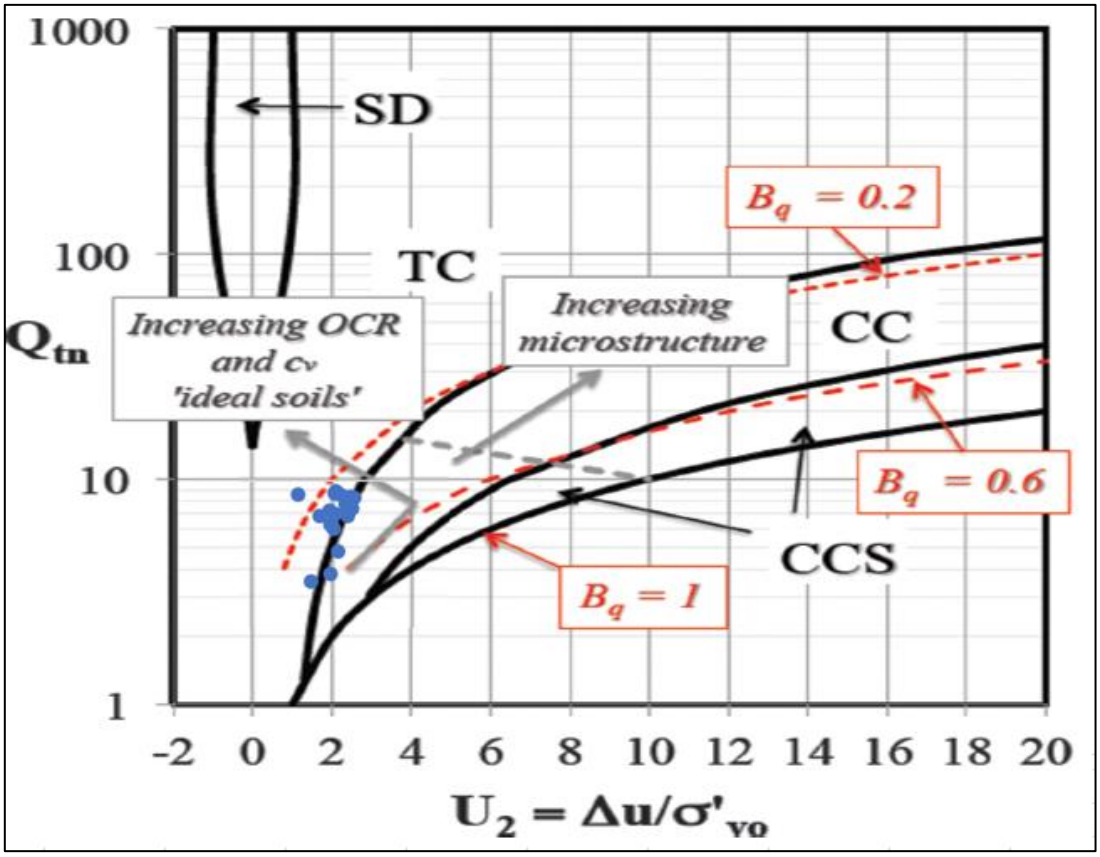

Figure 4.1: Updated: Q_t – U_2 plot developed by (Schneider et al., 2008) and updated by (Robertson, 2016), with points plotted representing the weak clay layer at Verdal Port. See key in Figure 4.2

The Q_{tn} – U_2 classification chart from SBTnm (2010) displayed in figure 4.1 indicated that the weak clay encountered at Verdal Port is on the border between clay-like, contractive and sensitive (CCS) and transitional contractive (TC), with half CPTU data points falling within each of the two zones. The Q_{tn} – F_r plot displayed in figure 4.2 indicated that all the CPTU data points for the weak clay layer fall into the CCS zone, with one exception within the clay-like contractive zone (CS).

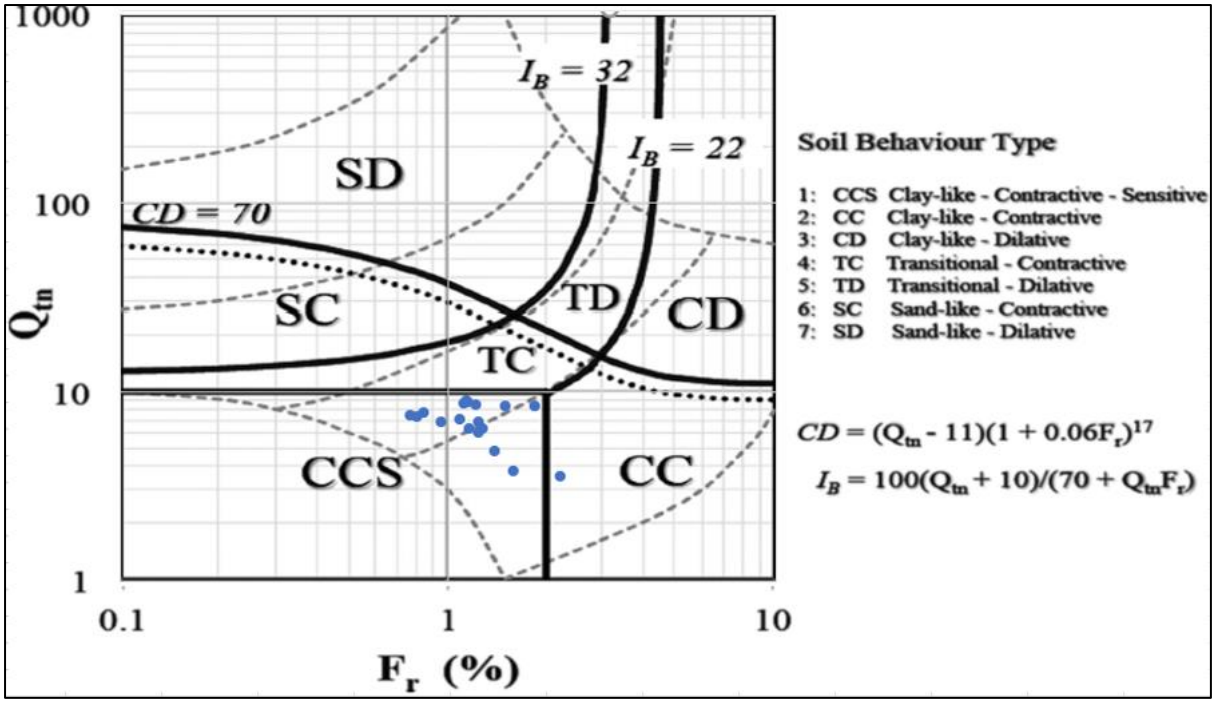

Figure 4.2: The $Q_{tn} - F_r$ plot shows the weak clay layer at Verdal Port exhibits clay-like, contractive, and sensitive behaviour with all but one of the CPTU measurements within the clay layer falling in the CCS zone

4.3 Discussion

If the weak clay layer at Verdal Port is indeed an event bed formation like those observed in (Hansen, 2011, L'Heureux, 2011, L'Heureux, 2012). Then we would expect this weak clay layer to have a honeycomb microstructure. Although the SBTnm results do not suggest that the weak clay has a high degree of microstructure, it is possible that the honey-comb microstructure is present. This is possible because the honeycomb microstructure is common in recent clay sediments (Sergeyev et al., 1980) and displays the lowest strength and highest degree of openness of all microstructures investigated in (Sergeyev et al., 1980). This could be the cause of the lower values of Q_{tn} and U2 observed in our results as Q_{tn} decreases with strength while U2 decreases with openness.

However, it is not possible to reliably assess the presence of microstructure based on standard CPTU measurements alone. To get a true idea if microstructure is present within the weak clay SCPTU investigations would be required. (Eslaamizaad and Robertson, 1996) and (Schnaid, 2009) have suggested that SCPTU can be used to identify microstructure within soils, by using shear wave velocities to calculate the small shear strain modulus. (Schneider and Moss, 2011) developed a chart to identify the presence of microstructure in soils, based on empirical correlations which were extended by (Robertson, 2016), this chart is displayed in figure 4.3.

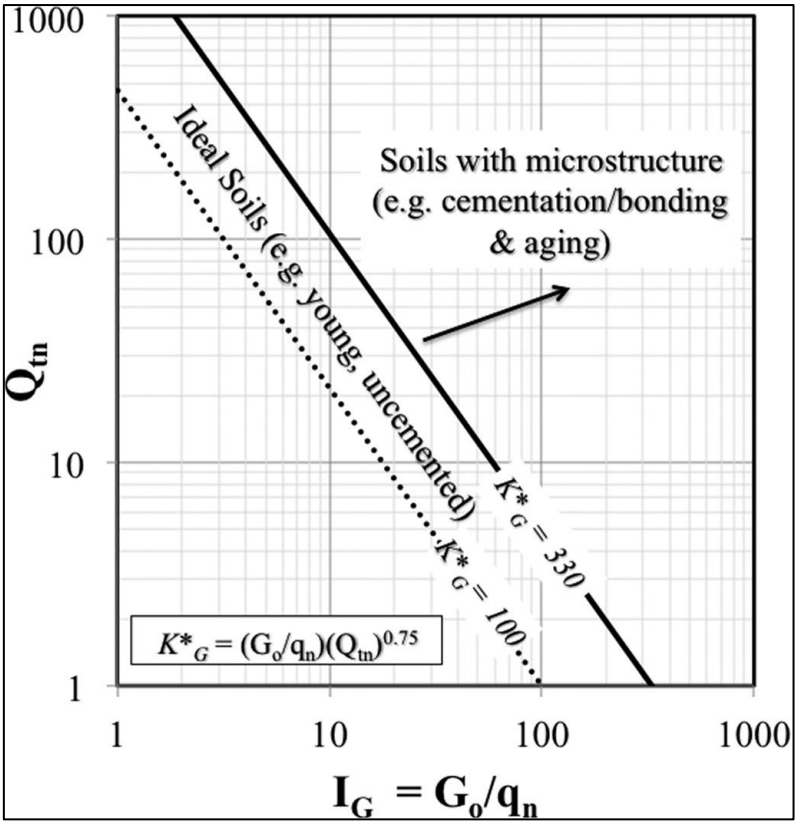

Figure 4.3: Chart to identify microstructure in soils by (Schneider and Moss, 2011) and extended by (Robertson, 2016)

The positive U2 values obtained by the CPTU suggest a contractive failure of the weak clay will occur at large strains (Robertson, 2016). Contractive failure behaviour at high strain is commonly observed in normally consolidated clays.

The modifications to the (Robertson, 2016) SBTnm classification charts make them more reliable than the SBTn (Robertson, 1990) classification, as pore pressure is given as U2 rather than B_q (Schneider et al., 2008). In addition, the Q_{tn}-F_r chart has been updated to give a better indication as to whether contractive or dilative behaviour will occur within a soil at high strains. These modifications allow the SBTnm scheme to provide better information into how soil behaves at high strains and observe any influence microstructures may have on the geotechnical behaviour of the soil.

The stability back analysis performed for the Verdal Port slide is a limit equilibrium analysis and therefore another advantage of the SBTnm classification is that it provides more detailed information on the mechanism of the soil failure. For these reasons it is interpreted that the SBTnm classification method provided the most reliable SBT classification from CPTU data for this investigation.

Therefore, the PLAXIS 2D models that use SBTnm based soil profiles were probably the best to use for the finite element slope stability back analysis, because theoretically, these models should return the most reliable results. However, even though the SBTnm has been improved there is still a high degree of uncertainty associated with CPTU soundings. Therefore, it is recommended that geotechnical investigations for high-risk projects should also encompass other field and laboratory investigation.

5. Finite Element Modelling, PLAXIS 2D

5.1 Model Construction

For the finite element modelling, the software PLAXIS 2D was used. In PLAXIS 2D plane strain models were developed with 15 noded elements, with very fine meshes used. The Mohr-Coulomb criterion was implemented for the determination of the strength parameters. Staged construction was used to alter input parameters of the weak clay layer systematically to investigate several different scenarios of variable geotechnical conditions.

Due to the variation in the resulting soil profiles constructed from multiple SBT classification schemes, it was uncertain if the thin clay layer was continuous or if it pinched out at some point between CPTU 1 and CPTU 2, and the thickness of the clay layer also varied depending on which SBT chart was used. Therefore, three models were produced, one for each SBT classification scheme. The soil profiles constructed from the SBT classification schemes, SBT (Robertson, 2010), SBTn (Robertson, 1990) and SBTnm (Robertson, 2016) were imported into PLAXIS 2D.

The soil profiles were simplified to include a sand layer, which was assumed to behave in a fully drained manner. This sand layer encompassed a softer weaker clay layer through which failure is thought to have occurred. The weak clay was modelled as a fully undrained material. As there was no data available on the stiffness of the soils, standard values based on previous experience were assumed. These values were E = 12.8 Mpa for the sand layers and E_u = 3.62 MPa for the weak clay layer.

Once the most likely geological structure and failure mechanism were determined from the PLAXIS 2D models, further finite element analyses were conducted. The aim of these further investigations was to investigate the uncertainties associated with the CPTU interpretations of clay layer angle and thickness and tidal influences on slope stability. Finally, the slope stability back analysis was used to estimate the undrained strength parameters of the weak clay soil.

Although it is suggested in the previous chapter that the SBTnm charts theoretically provide the most reliable SBT classification, all three SBT, SBTn and SBTnm soil profiles were investigated during different parts of the finite element investigations. This was conducted to gauge how differences in SBT zone interpretations can affect slope stability assessment.

5.2 Clay Lateral Extent and Failure Mechanism

5.2.1 Method

To investigate the most likely horizontal extent of the weak clay layer, staged construction was used in PLAXIS 2D to try different scenarios where the clay layer terminated at different x-coordinates throughout the SBT, SBTn and SBTnm models.

The SBT soil profile indicates that the weak clay layer is present at a depth of 3.59 m – 3.83 m at CPTU 1 and this layer gets thinner towards CPTU 2 where it is present at a depth of 4.83 m–4.85 m. The SBT profile feasibility was therefore investigated with the clay layer persisting throughout the entire horizontal extent of the model, as well as terminating at points beyond CPTU 2. The mesh and scenarios for this model are displayed in figure 5.1.

This analysis was performed for the three possible scenarios implied by the SBT CPTU profile which were:

- Clay extending throughout the entire model.
- Clay pinching out adjacent to CPTU 2.
- Clay thinning from CPTU 1 to CPTU 2 and then pinching linearly past CPTU 2, assuming the same rate of decreasing thickness as observed between CPTU 1 and CPTU 2.

Similar investigations were performed using the SBTn and SBTnm models. However, these models used different clay geometry scenarios, as the SBTn and SBTnm profiles both indicated that the weak clay layer is present at CPTU 1 but terminates at some point before CPTU 2. The mesh for the SBTnm model, with indicators of the clay termination points used, are displayed in figure 5.2. The SBTn model used the same clay termination x-coordinates as the SBTnm model because the principal difference between the SBTn and SBTnm soil profiles was the thickness of the weak clay layer, this difference is described in more detail in section 5.4. The several possible scenarios implied by the SBTn and SBTnm profiles (figure 5.2) were modelled with the clay pinching out at x-coordinates of 119.03, 120.95, 123.50, 124.00, 126.00 and 128.00.

To identify the most likely soil stratigraphy from the SBT, and SBTn, SBTnm models that were produced, and to better constrain the lateral extent of the weak clay layer, an approximation of the post-failure seabed morphology, which was based on geophysical data and the previous slope stability investigations in (Hundal and Øiseth, 2019, Moholdt, 2019), was correlated to the incremental displacements results from the PLAXIS 2D models.

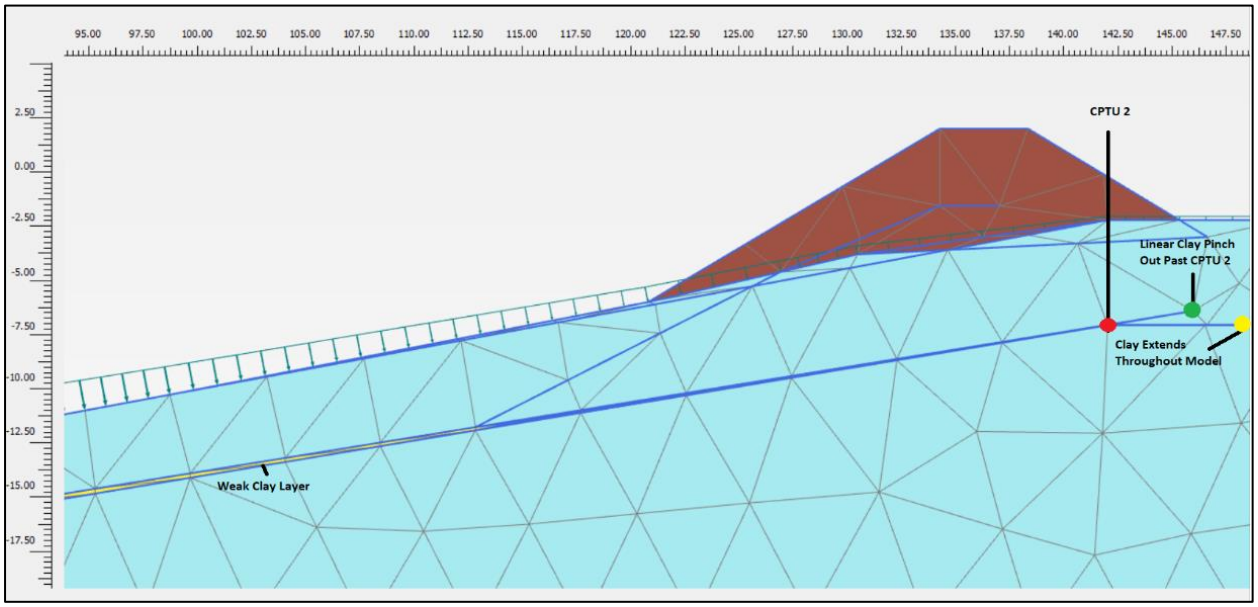

Figure 5.1: Mesh from SBT models showing the weak clay termination points for each possible scenario. Clay Terminating at CPTU 2 (red), Clay thinning linearly past CPTU 2 (green) and Clay extends throughout the entire model (yellow)

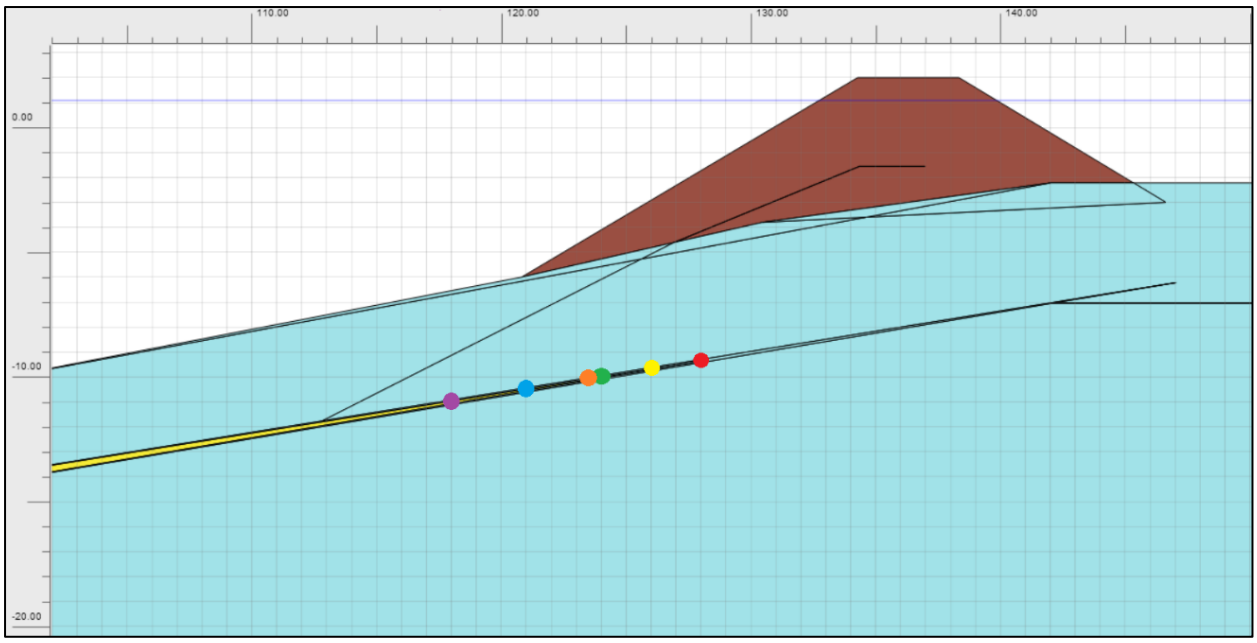

Figure 5.2: Mesh from SBTnm model showing the weak clay termination points for each possible scenario. Clay Terminating at x co-ordinates 119.03 (purple), 120.95 (blue), 123.50 (orange), 124.00 (green), 126.00 (yellow) and 128.00 (red). The same scenarios and x co-ordinates for clay termination point were also used for the SBTn model

The incremental displacement plots from the PLAXIS 2D models are useful to observe the localities where deformation occurs as the soil fails, and are therefore indicative of a most likely failure mechanism (PLAXIS, 2018). Therefore, the scenarios that gave a failure mechanism correlating best with the post-failure topography were interpreted to be the most likely soil profiles.

5.2.2 Results

The incremental displacements for the three clay geometries analysed in the SBT models have been displayed in figures 5.3, 5.4 and 5.4. These were very similar to each other, suggesting that once the clay layer extends to CPTU 2 there is little change in the failure mechanism, regardless of how far to the weak clay layer extends past the locality of CPTU 2. The results from all three of the SBT models did not correlate well with the post-failure bathymetry, as the suggested failure mechanism for these models proceeds further to the right, beneath the constructed fill. The displaced mass was also very restricted and did not travel far in the downslope direction.

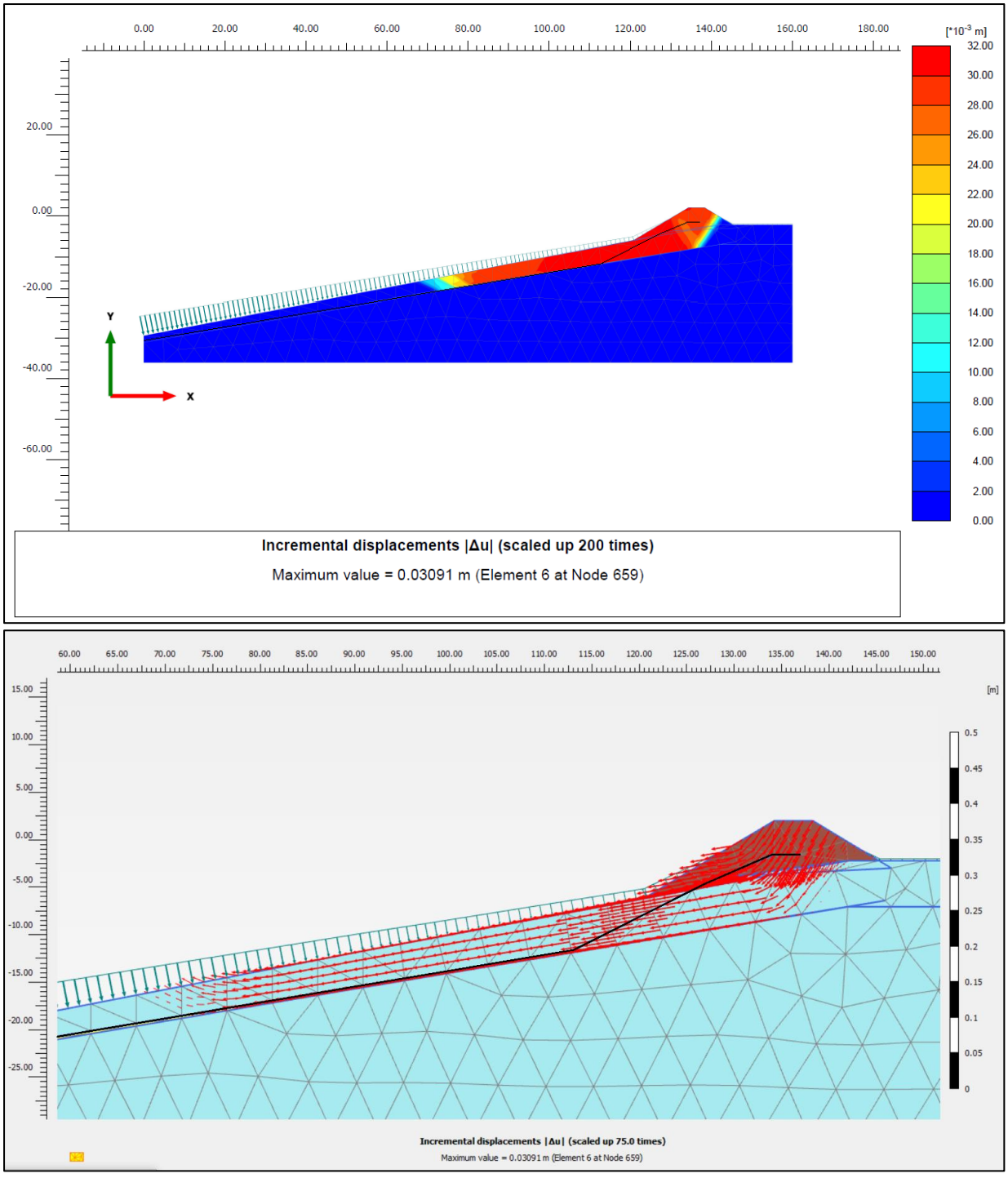

Figure 5.3: Incremental displacement plots for continuous clay layer, (SBT Profile). Approximate post-failure terrain is indicated by the black line

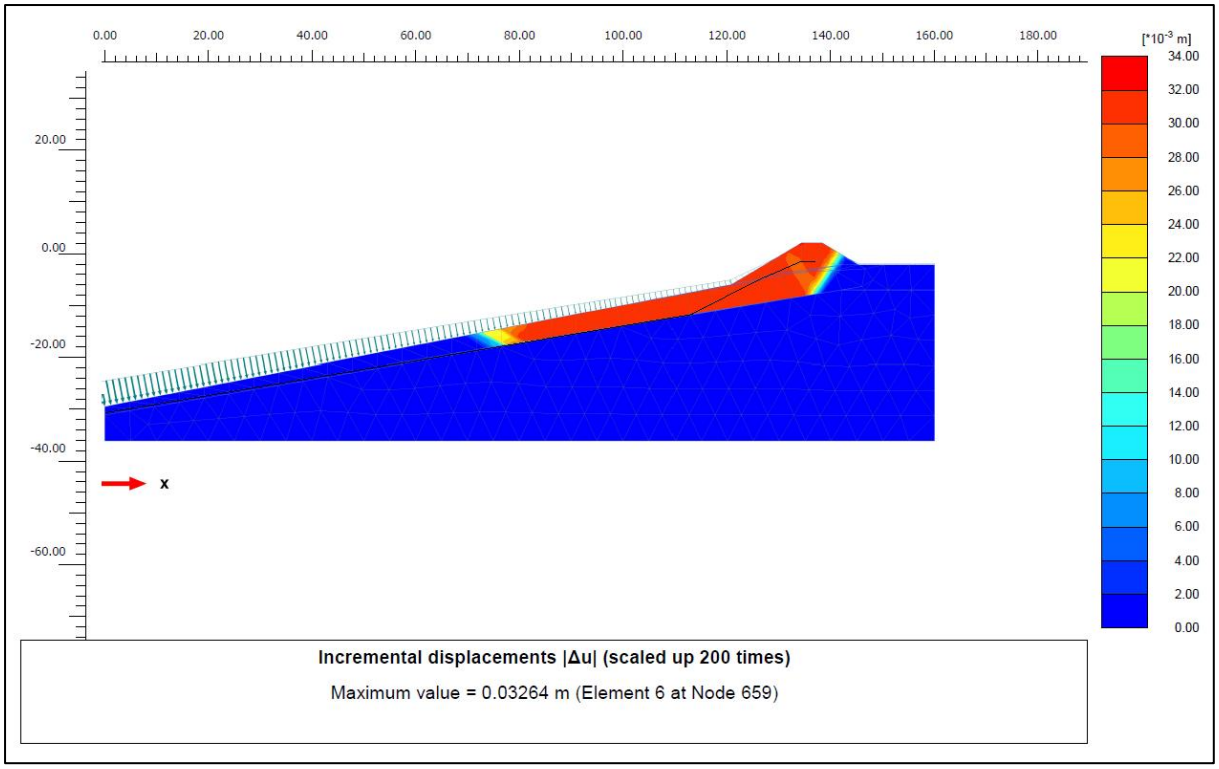

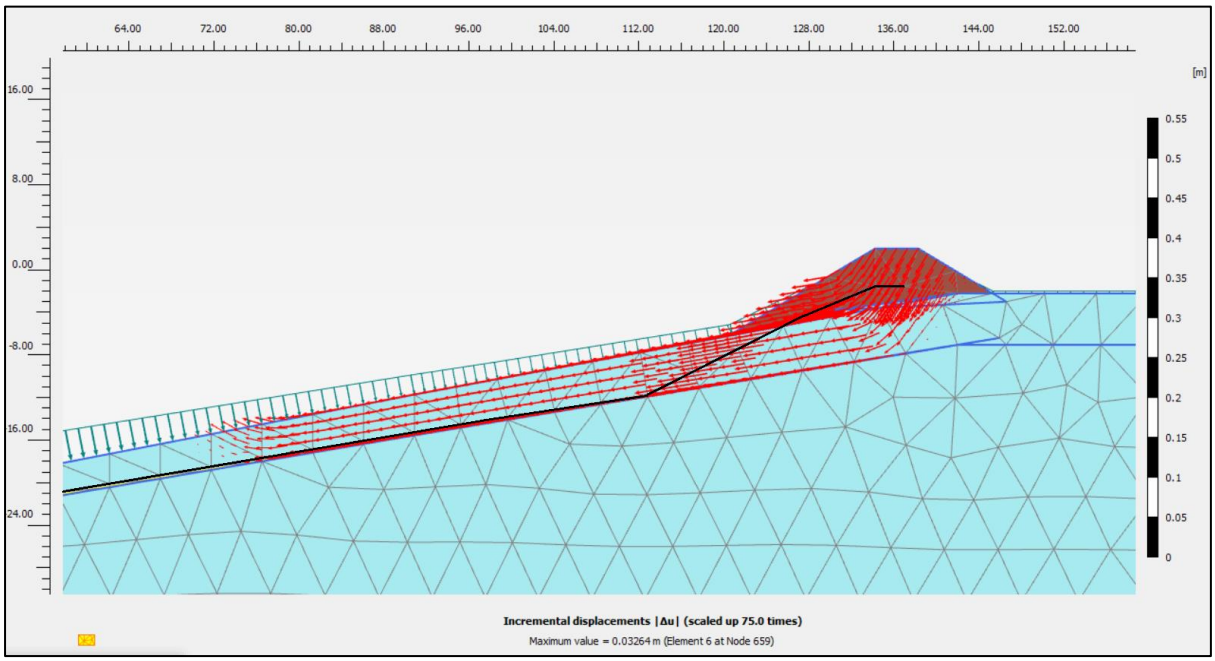

Figure 5.4: Incremental displacement plots for the clay layer pinching out adjacent to CPTU 2, (SBT Profile). Approximate post-failure terrain is indicated by the black line

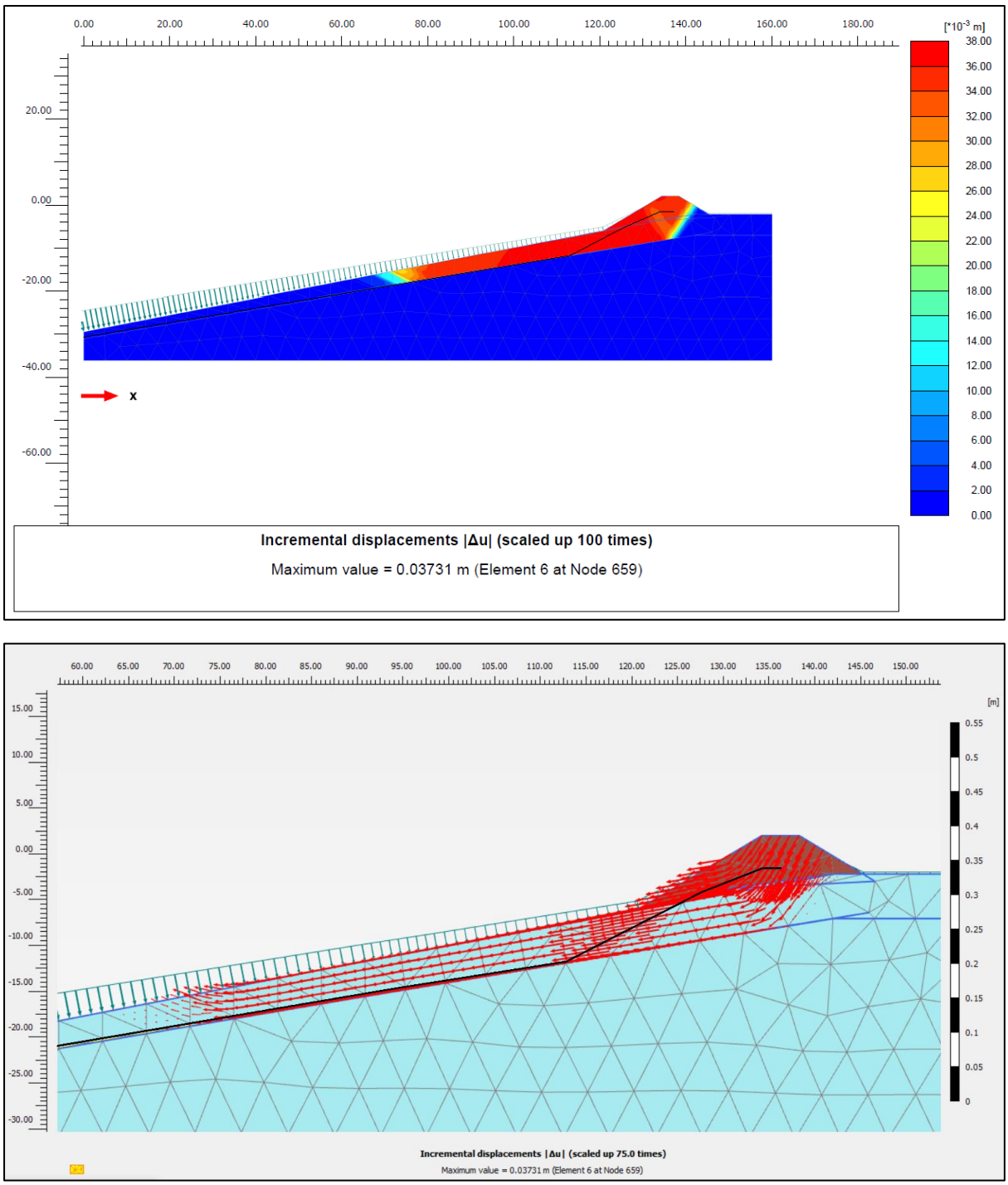

Figure 5.5: Incremental displacement plots for clay layer pinching out at linear rate past CPTU 2, (SBT Profile). Approximate post-failure terrain is indicated by the black line

The incremental displacement results for the SBTn and SBTnm models were similar but suggested that there were significant differences in the development and location of the failure surface, depending on the lateral extent of the weak clay layer. The models in which the weak clay layer pinched out at x-coordinates of less than 121 did not correlate well to the post-failure bathymetry as they showed landslide development too far to the left of the fill. Results from all SBTnm scenarios used in this analysis are presented in Appendix A. The SBTnm and SBTn models in which the weak clay layer terminates over an x-coordinate range of x = 123.5 – 126 indicated a landslide failure mechanism that correlated better with the post-failure bathymetry observed at Verdal Port.

The SBTnm model with the weak clay layer pinching out at x = 124 displayed the best fit for both the SBTn and SBTnm models when correlating the failure mechanism suggested by incremental displacements to the post-failure bathymetry. The SBTn and SBTnm models with clay termination at x = 124 are displayed in figures 5.6 and 5.7.

The principal difference between the incremental displacement results from the SBTn and SBTnm models was the length over which the soil displacement occurs, with the SBTn showing more restricted displacement while the SBTnm shows displacement extends much further downslope.

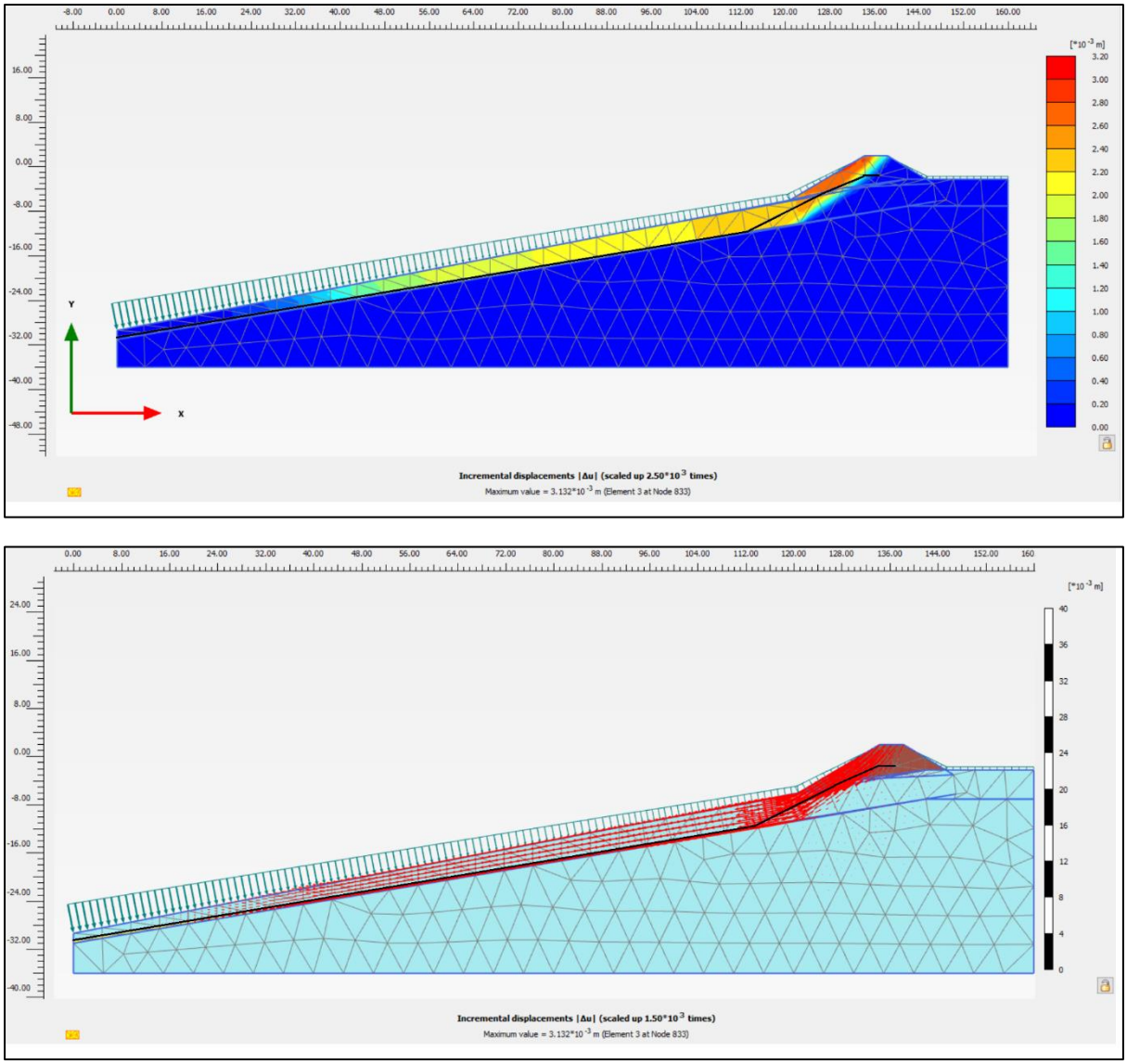

Figure 5.6: Incremental displacement plots for clay layer pinching before CPTU 2 at x =124, (SBTnm Profile). Approximate post-failure terrain is indicated by the black line

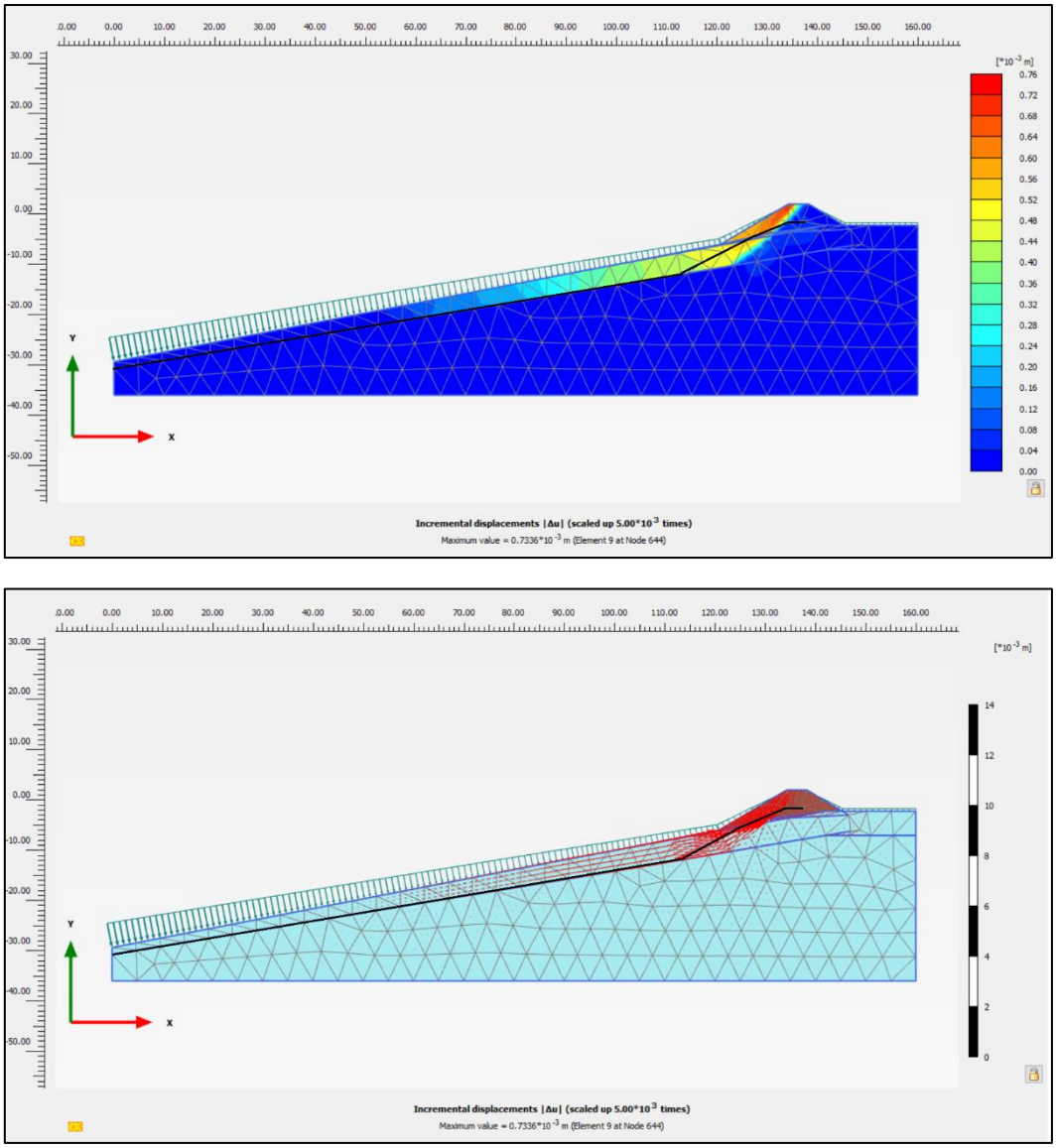

Figure 5.7: Incremental displacement plots for clay layer pinching before CPTU 2 at x =124, (SBTn Profile). Approximate post-failure terrain is indicated by the black line

5.2.3 Discussion

The SBT profile, which indicated that the clay layer persists past CPTU 2, is less likely as the correlation between the post-failure terrain level and plots of incremental displacements in the models suggested that the clay layer most likely pinched out at a point before CPTU 2.

The incremental displacement and post-failure bathymetry correlations from the SBTnm models were consistent with that of the SBTn models in indicating that the weak clay layer does not extend past CPTU 2. This further constrained the geometry of the weak clay layer suggesting that the SBTnm and SBTn models, where the clay pinches out within the range of x = 123.5 – 126 were the most likely clay layer geometries for the Verdal Port slope.

The SBTnm soil profile has been interpreted as more reliable than the SBTn model as the soil displacement extended much further downslope, which is in line with what was expected, based on observations of the post-failure bathymetry. The increased lateral displacement of soil, exhibited in the incremental displacement results for the SBTnm model, was most likely due

to the fact that increases in the thickness of weak soil layers result in increased displacement of the failure mass (Liu and Koyi, 2013).

In addition, the very thin nature and negative CPTU side friction values at 3.95 – 3.97 m, mentioned previously, introduced an even higher degree of uncertainty when using the SBTn classification to interpret the weak clay layer. Therefore, the SBTnm model with the clay layer terminating at x = 124 gave the best fit and has been interpreted to be the most likely soil profile.

However, even though a most likely range and the best fitting model has been identified from these results it should be noted that there are unknown factors that may lead to inaccuracies in this analysis. For example, we know the post-failure terrain based on bathymetric data supplied in (Moholdt, 2019), however, this was taken shortly after failure. Therefore, it is possible that some landslide debris settled immediately following the submarine landslide. Hence, the actual failure surface could be lower than the terrain level indicated by the bathymetric measurements. The difference in bathymetric elevation due to this immediate settlement is likely to be small, and the associated uncertainty has been partially accounted for by providing a range of feasible clay layer geometries, rather than a single measurement.

The actual orientation and changes in the thickness of the clay layer downslope from CPTU 2 are also unknown, as no geotechnical soundings were conducted in this area. The influence that these uncertainties may have on the results were investigated in further detail in chapter 5.3 and 5.4.

5.3 Clay Angle Effects

5.3.1 Method

There were no geotechnical drilling investigations conducted in the downslope direction from CPTU 1, therefore, the actual angle of the weak clay layer is uncertain past this point. Comparisons between the pre-failure and post-failure seafloor morphology show that the thickness of the displaced soil is relatively constant along most of the slope, with a slight decrease in thickness at the sections furthest downslope from the fill. Although this suggests that the weak clay layer is at a relatively constant depth throughout the slope, it should be noted that the post-failure bathymetry is not linear and has small undulations, it should also be noted that post-failure bathymetry does not necessarily represent the exact landslide failure surface because there may have been settlement immediately after the landslide occurred, before bathymetry measurements were made. Therefore, the post-failure bathymetry is only a rough indicator of the landslide failure surface.

To investigate the impact these sources of error may impose on the slope stability analysis different SBTnm models were created with slight variations in the angle for weak clay layer for the section downslope from CPTU 1. The angles of the clay layer downslope from CPTU 1 that were used in this investigation were: 11.42°, where the angle is equal to the post-failure slope, 9.5°, where the angle is slightly less than the post-failure slope angle and 13.34°, where the clay layer angle is slightly greater than the post-failure angle of the slope. The S_u values required to achieve a FS = 1 were then recorded for each model to assess the impact the clay layer angle had on slope stability. For simplicity, only the high tide and low tide SBTnm models and their corresponding S_u results were analysed in this investigation.

All the models produced were analysed and interpreted to decide which geological profile was most likely and correlated best with the post-failure terrain level, while also producing feasible results for the strength parameters of the weak clay.

5.3.2 Results

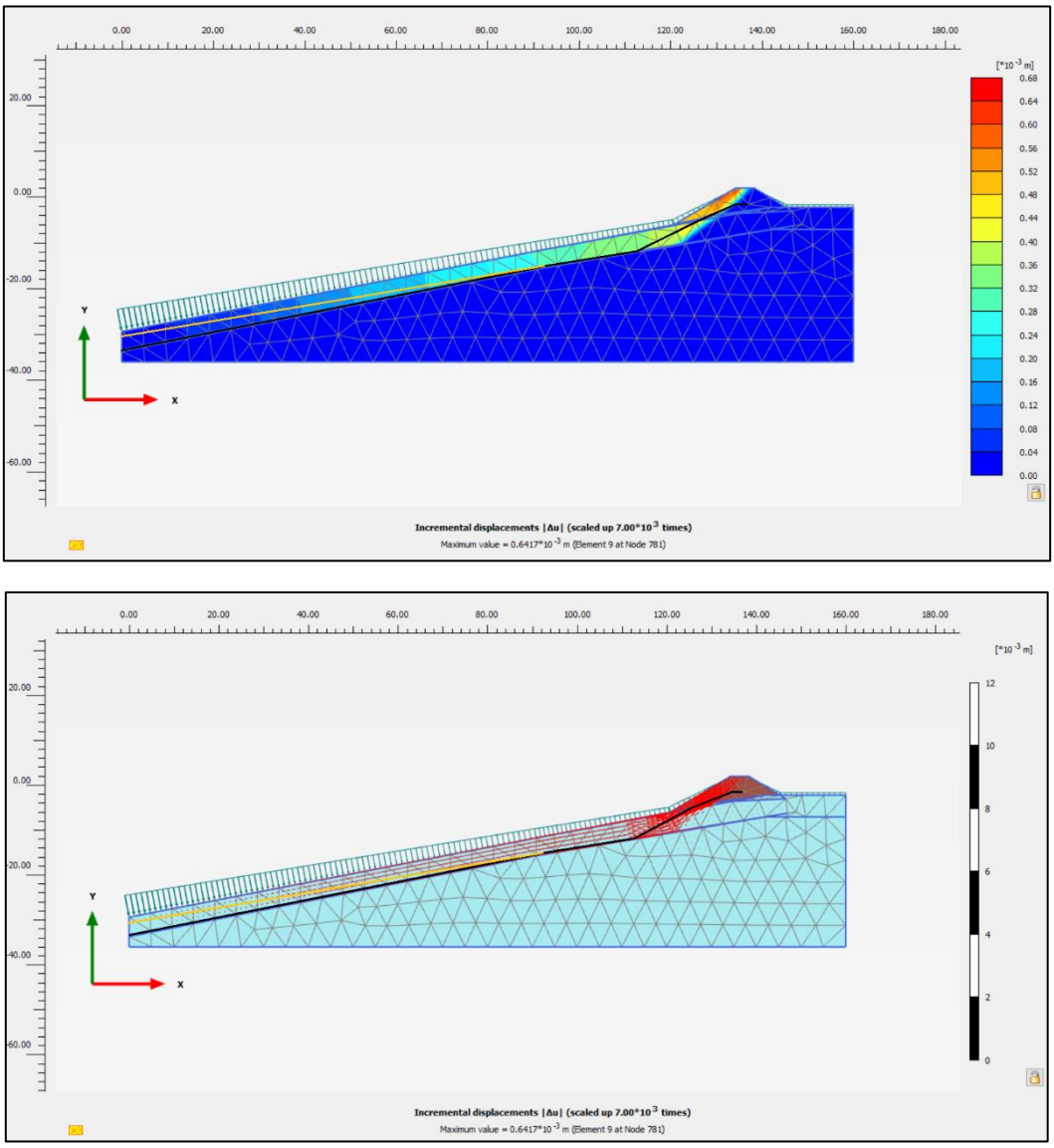

Figure 5.8: Incremental displacement plots for clay layer termination at x =124, SBTnm model. Clay angle is modelled downslope from CPTU 1 as 11.42°, which is equal to the slope angle. Expected failure surface is indicated by the black line, the approximated true post-failure bathymetry downslope of CPTU 1 is indicated by the yellow line

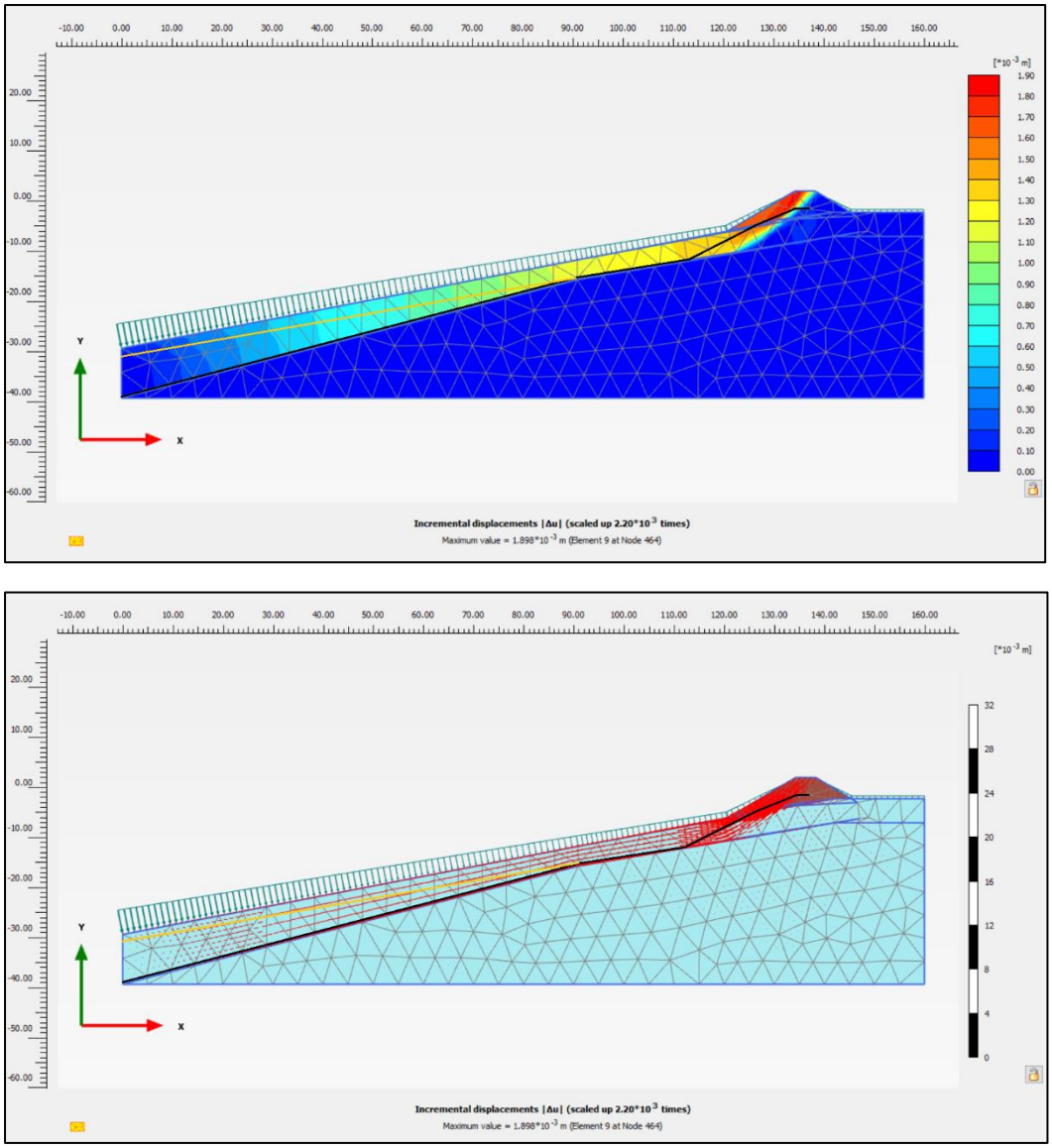

Figure 5.9: Incremental displacement plots for clay layer termination at x =124, SBTnm model. Clay angle is modelled as 13.34° downslope from CPTU 1. Expected failure surface is indicated by the black line, the approximated true post-failure bathymetry downslope of CPTU 1 is indicated by the yellow line

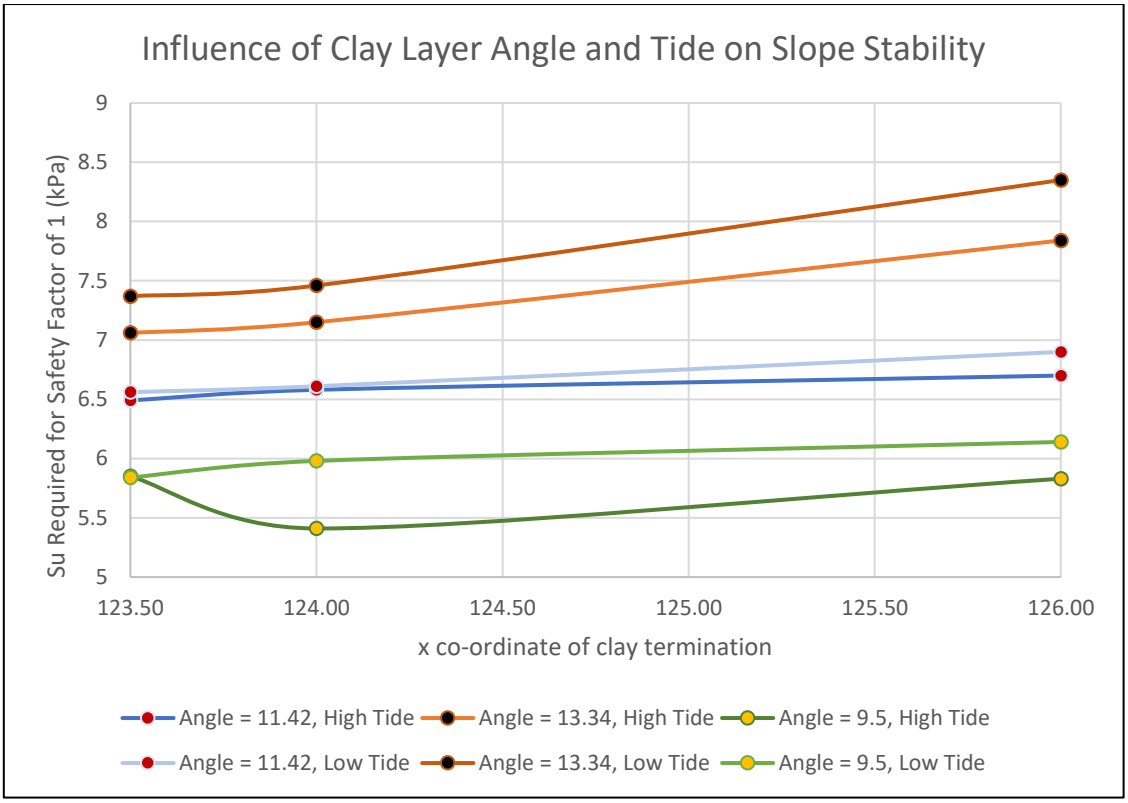

Figure 5.10: S_u as a function of clay layer angle for SBTnm models. Both high and low tide results

In general, as the angle of the clay layer increased the required S_u to obtain a factor of safety above one also increased. It is shown in figure 5.10, that altering the weak clay layer by just 1.92° can result in a required increase of S_u of up to 1.45 kPa to achieve a factor of safety equal to one.

5.3.3 Discussion

The clay layer angle of 9.5° downslope from CPTU 1 provided the best correlation to the approximation of the true post-failure terrain, as the thickness of displaced material tended to decrease slightly downslope from CPTU 1. However, the model with a clay layer angle of 11.42° also correlated reasonably well with the post-failure terrain, even though the failure surface suggested by this model is slightly deeper. It is likely that there was some immediate settlement of landslide debris that was displaced during the failure. This suggests that the actual failure surface may be at a greater depth than the post-failure terrain level and therefore clay layers angles of 9.5°, 11.42° and 13.34° are all feasible.

There is a high degree of uncertainty pertaining to the actual angle of the weak clay layer because no geotechnical soundings were carried out downslope of CPTU. Hence, it was impossible to reliably identify the pre-failure geological structure of the sediments in this section of the slope. The results in figure 5.10 indicated that even small changes in the angle of the weak clay layer downslope from CPTU 1 had significant impacts on the strength parameters derived from the slope stability analysis. To reduce this source of error and make a more accurate assessment of the clay layer angle, further pre-failure geotechnical investigations

such as additional CPTU soundings would be required. However, the finite element analysis and post-failure seabed surface allow us to make an estimate based on geotechnical judgement.

5.4 Influence of Clay Thickness on Stability

5.4.1 Method

There have been a very limited number of studies conducted to assess the role that weak layer thickness plays in respect to slope stability (Liu and Koyi, 2013), and no studies were found which analyse the influence weak layer thickness has on the stability of submarine slopes.

Systematic slope modelling conducted by (Liu and Koyi, 2013) found that increases in weak layer thickness result in increased displacement of the failure mass, while results in (Crusoe-Jr et al., 2016) have shown "As the weak layer thickness increases from a lower value to a higher one, the safety factors occur in a variation process from a low decline to an accelerated decline and back to a slow decline". These studies suggest that increases in weak layer thickness are generally accompanied by decreases in the overall stability of the slope.

The main difference between the SBTn and SBTnm profiles is the differences in the thickness of the weak clay layer at CPTU 1. The SBTn model suggested that the clay is just 2 cm thick at CPTU 1, while the SBTnm suggested a thickness of 38 cm. This is a significant difference and highlights the uncertainties involved in producing soil profiles from the Robertson SBT classification charts.

To help quantify the impact of the uncertainties associated with the clay thickness on overall slope stability, we have produced several models with varying thicknesses of the clay at CPTU 1. All these models have the same lateral extent of clay with this weak layer terminating at an x-coordinates of 124. Using the SBTnm model, the thickness of the clay at CPTU 1 was systematically varied, ranging from 1 cm to 100 cm, to assess the impact that the clay thickness had on the factor of safety for the slope.

5.4.2 Results

The results from the clay thickness analysis have been displayed in figure 5.11. These results were in line with what was found in (Crusoe-Jr et al., 2016), with a general decrease in the factor of safety as the clay layer thickness increased from 8 cm to 100 cm, the rate at which the safety factor decreased was variable across this range of thickness.

However, the relationship between the thickness of the weak clay layer and safety factor for weak layer thickness less than 8 cm indicated this trend was not consistent for very thin weak layers. In this thin range of thickness, it is obvious that the trend direction was reversed, with decreasing thickness of the weak layer resulting in a decreasing factor of safety. The magnitude of the changes in safety factor over this range was also much greater than for the thickness range above 8 cm.

From figure 5.11, it is recognised that the most critical stability scenario was when the clay layer has a thickness of 1 cm, while the greatest stability was achieved when the weak clay layer has a thickness of 8 cm.

The weak clay thickness of 2 cm suggested by the SBTn model gave a factor of safety of 1.158, while the SBTnm derived clay thickness of 38 cm produces a factor of safety of 1.209.

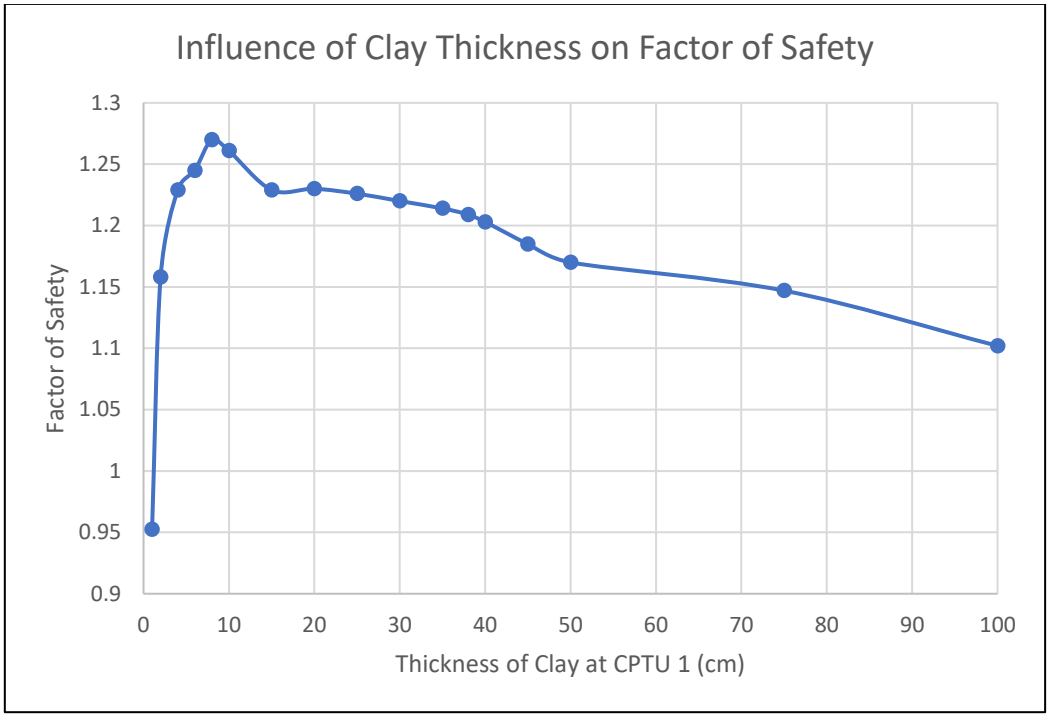

Figure 5.11: The relationship between the thickness of the weak clay layer and the factor of safety of the Verdal Port slope

5.4.3 Discussion

From the results of the weak clay layer thickness analysis, it is observed that the thickness had a significant outcome on the overall stability of the slope. The studies from (Liu and Koyi, 2013) and (Crusoe-Jr et al., 2016), which suggested a decreasing slope safety factor as the weak layer thickness increased, did not analyse the impact weak layer thickness had on slope stability for any weak layer thickness below 10 cm. This is critical as it has been shown that the safety factor trend was in the opposite direction and of greater magnitude when the weak layer thickness was in the range of 1 cm – 8 cm. This is critical with respect to the stability of slopes which contain thin weak layers with thicknesses below 8 cm, as variations in thickness within this zone tended to have the greatest effect on the factor of safety of the slope.

For the Verdal Port, this is important as the SBTn profile indicated a clay layer thickness of 2 cm at CPTU 1, while the SBTnm profile indicated a thickness of 38 cm at CPTU 1. Therefore the two SBT classification schemes produced results that were highly variable when compared to each other, with the difference in the weak clay layer thickness between the two being 36 cm. Therefore, stability analyses will be greatly impacted by which Robertson SBT classification scheme is utilised, especially in soils which have an abundance of thin layers. Further research is needed to investigate the mechanisms related to decreasing stability when the weak layer thickness is between 1–8 cm. This further highlighted the uncertainties associated with using CPTU measurements and SBT classification to produce soil profiles.

5.5 Tidal Contribution to Instability

5.5.1 Method

For the Verdal Port landslide, it was noted that the failure did not occur immediately during the construction of the fill, rather, the submarine slope failed at some time after construction had finished for the day. Hence, the slope failure was not identified until the next day. This delay in failure suggests that a progressive, strain-softening failure mechanism was possible. However, it is also likely that this delayed failure was due to tidal influences facilitating a dynamic sea water level, which would have had a significant impact on the slope stability.

The external water level has a significant influence on the stability of waterfront slopes (Johansson and Edeskär, 2014), one reason for this is due to the fact external water pressure provides a stabilising force to these types of slopes (Duncan and Wright, 2005). The primary causes for water level fluctuation in such cases are waves, heavy rainfall events, snowmelt and tidal variations. Because the Verdal Port is relatively sheltered, the fluctuation of external water is assumed to have had minimal impact from waves. No heavy rainfall events or snowmelt occurrences were recorded prior to the slope failure, so these factors have also been assumed to have a negligible impact on the slope stability at Verdal Port. For these reasons it has been assumed that the primary influence on external water pressure for the slope at Verdal Port is tidal variation.

As the water level is lowered by tidal processes the hydraulic gradients may be altered to induce seepage forces within soils that are below the water level initially, but move above the water level as the tide drops (Johansson and Edeskär, 2014). This seepage results in the soils involved being subjected to water flow forces that can also have destabilising effects on slopes and can induce erosion. However, the only material that could have been subjected to seepage in the case of the Verdal Port landslide is the fill material. However, the geotechnical properties of the fill material and finite element models suggested that failure of the fill due to seepage was unlikely.

With the previous points in mind, the reduction of the water level due to tidal fluctuation has been identified to destabilise the slope in two ways, by reducing the stabilising force provided by the external water pressure and by increasing the effective stresses imposed on the thin clay layer by the fill material.

The high and low tide elevation for sea levels for the dates 8th and 9th January 2019 were determined using tidal records from www.kartverket.no, these records are presented in Figure 5.12 and indicated that the water level fluctuated between +1.09 m at high tide to -1.16 m at low tide.

Therefore, to investigate, the impact of tidal influence on slope stability the water levels were altered from +1.09 m to -.1.16 m using the SBTnm model with staged construction in PLAXIS 2D to see how the factor of safety for the slope changed with changes in sea level. The S_u required for a safety factor of one was also recorded during this analysis. To obtain a range of FS and S_u values and investigate how these values were influenced by the continuity of the clay layer, this analysis was conducted for each feasible clay geometry pinching out between x-coordinates of 123.5 – 126.

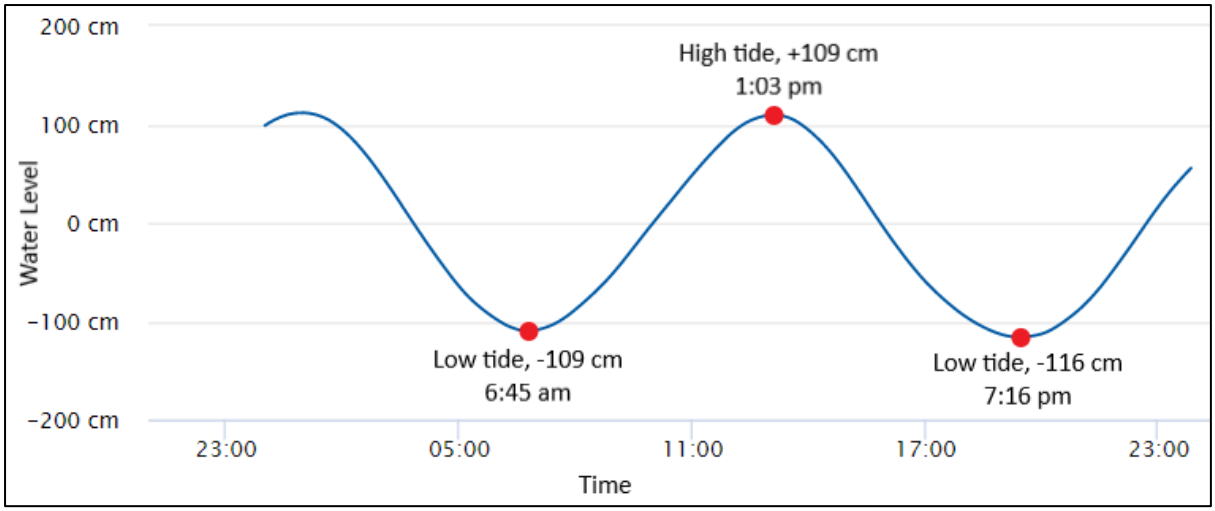

Figure 5.12: Plot showing high and low tide time and water level elevation in Trondheimsfjorden for 8th January 2019

5.5.2 Results

The results from this analysis into how tidal conditions may have influenced slope stability are displayed in table 5.1. In contrast to what was expected, some results indicated that the high tide conditions were more critical with respect to slope stability, with slightly higher S_u values required to reach a safety factor of 1. The differences in S_u required for high and low tide were very small in these models, ranging from 0.02 to 0.17 kPa. In contrast, the models where the clay terminated at an x-coordinates greater than 123.5 indicated the low tide conditions were more critical, with higher S_u values required at low tide to achieve a safety factor of one. The models where the clay terminated at a point greater than x = 123.5 displayed greater differences between the Su values required to achieve safety factors equal to 1, with the differences in S_u ranging from 0.31 to 0.57 kPa. The best fit model, where the weak clay layer terminated at x = 124 gave an S_u = 5.41 kPa for high tide and an S_u of 5.98 kPa for low tide.

Clay Termination x coordinates	S_u for FS = 1 (High Tide)	S_u for FS = 1 (Low Tide)	S_u Change
119.03	5.1	4.93	0.17
120.95	5.57	5.55	0.02
123.50	5.85	5.84	0.01
124.00	5.41	5.98	0.57
126.00	5.83	6.14	0.31
128.00	6.65	6.98	0.33

Table 5.1: Tidal analysis results using the SBTnm model, S_u is given in kPa

5.5.3 Discussion

The results from the tidal analysis indicated the tide has some influence on the factor of safety and hence the stability of the Verdal Port slope. The magnitude of changes in the factor of safety due to tidal fluctuations was more significant in the models that suggested that low tide conditions were most critical with respect to slope stability.

For the x = 124.00 SBTnm model that has been interpreted to most likely represent the actual soil profile, the low tide conditions required an S_u 0.57 kPa greater than that required in high tide conditions. These findings suggest that it is possible that the tidal fluctuations may have contributed to the delayed failure that was witnessed at Verdal Port and this is supported by the timing of the tides on 8th January 2019. It is likely that when the fill construction had finished for the day the tide was at an elevation significantly higher than the low tide mark. The tidal records from www.kartverket.no indicated the most critical tide conditions at low tide took place at 7:16 pm, at which time construction would have finished for the day, this could at least partially explain the delayed slope failure and why the submarine landslide was not observed until the next day.

Therefore, it is feasible that the tides may have triggered the Verdal Port landslide, especially if the shear stress imposed on the sediments by the newly constructed fill was close to the S_u of the weak clay layer when fill construction ceased for the day. However, it is also possible that the delay in failure was due to strain-softening progressive failure. It may have also been a combination of both these factors.

There were several limitations to this tidal investigation as we did not know the exact time of the Verdal Port landslide, hence, the actual sea elevation at failure was also unknown. This analysis only looked at the most critical and most stable tidal conditions. Also, when using PLAXIS 2D to model very small changes in the safety factor and S_u, PLAXIS 2D gave inconsistent results as the resolution was not high enough to accurately assess such small variations. Furthermore, progressive failure analysis would be required to identify if this phenomenon also played a role in the delayed failure. However, for this case, it was very difficult to make a reliable assessment of strain-softening behaviour because no deformation data was recorded prior to the Verdal Port landslide.

5.6 Strength Parameters Back Analysis

5.6.1 Method

For slope stability analysis it is vital to determine the soil strength parameters cohesion and friction angle for drained conditions and undrained shear strength for undrained conditions (Lian-Heng et al., 2016). These strength parameters may be determined by field and laboratory tests or by landslide back analysis. When a landslide occurs it provides an excellent opportunity to perform a back analysis, which provides an estimate of the geotechnical properties pertaining to the soils in which the landslide has occurred (Gilbert et al., 1998).

The back analysis method has some advantages over laboratory methods as the soils in question are in-situ, time-consuming laboratory tests are not required and the scale encompasses the entire failure zone rather than individual samples from particular points (Gilbert et al., 1998). Therefore the back analysis technique can be used to reduce the dependency on laboratory tests for geotechnical investigations (Chandler, 1977).

(Gilbert et al., 1998) and (Lian-Heng et al., 2016) proposed that rather than a deterministic limit state back analysis using only mean strength parameters, a more probabilistic approach incorporating a range of possible strength parameters and failure mechanisms should be used to further reduce uncertainties associated with this method. Such probabilistic methods have been utilised for back analyses of slopes by (Gilbert et al., 1998). Taking this into account, the

S_u values determined by finite element analysis in this investigation have been used to produce a range of possible S_u values rather than a single value.

Once the finite element model geometries were established, the method of stability back analysis was used to estimate the undrained shear strength of the clay layer by systematically altering this parameter for each model and its stages until the models returned a factor of safety equal to 1. It should also be noted that the S_u was assumed to be constant even with increasing depth, this assumption was made because the clay layer is relatively shallow, thin and is situated at a relatively constant soil depth throughout the whole model. Therefore, even though we would have expected the S_u to increase with depth, the assumption of a constant S_u would have had a negligible impact on the results obtained from the finite element model. The S_u ranges provided for the weak clay layer also considered the tidal fluctuations occurring in the Verdal Port, where each scenario was given a low and high tide S_u value.

5.6.2 Results

A range of undrained shear strength values has been produced based on the finite element back analysis using the various SBTnm models which have been interpreted as more reliable than the SBT and SBTn models in regard to representation of the true soil profile.

These results are displayed in tables 5.2, 5.3 and 5.4. Overall, the range was from 5.41-8.50 kPa when considering influences from clay layer angle, tides, and the clay layer termination point. The range of S_u values for the best fit models, which have a weak clay layer termination point at x = 124.00 gave an S_u range of 5.41 – 7.46 kPa, with the low tide situations presenting the most critical conditions with regards to slope stability.

Clay Termination x Coordinates	S_u for FS = 1 (High Tide)	S_u for FS = 1 (Low Tide)
123.50	5.85	5.84
124.00	5.41	5.98
126.00	5.83	6.14

Table 5.2: S_u required to achieve a factor of safety greater than 1 as indicated by the SBTnm 9.5° model

Clay Termination x Coordinates	S_u for FS = 1 (High Tide)	S_u for FS = 1 (Low Tide)
123.50	6.49	6.56
124.00	6.58	6.61
126.00	6.7	6.9

Table 5.3: S_u required to achieve a factor of safety greater than 1 as indicated by the SBTnm 11.42° model

Clay Termination x Coordinates	S_u for FS = 1 (High Tide)	S_u for FS = 1 (Low Tide)
123.50	7.06	7.37
124.00	7.15	7.46
126.00	7.84	8.35

Table 5.4: S_u required to achieve a factor of safety greater than 1 as indicated by the SBTnm 13.34° model

5.6.3 Discussion

Studies by (Jamiolkowski et al., 1985) have determined that the undrained soil strength ratio (S_u /σ') for normally consolidated clay soils is typically within the range of 0.2 – 0.3 and that an average of 0.22 is often a reasonable assumption for such soils.

As discussed previously the SBTnm with clay layer termination at x = 124 has been decided as the most reliable SBT classification. While the x = 124 SBTnm model, with a clay layer angle of 9.5° provided the best fit with the post-failure bathymetry the S_u results of 5.41 – 5.98 kPa are lower than what would have been expected when compared to previous literature from (Jamiolkowski et al., 1985), as these values indicated an undrained soil strength ratio (S_u/σ') of 0.15 – 0.18.

The SBTnm models with the clay layer angle at 11.42° and 13.34° downslope from CPTU 1 gave undrained soil strength ratios closer to what we would expect with ranges of 0.18 – 0.20 and 0.21 – 0.23, respectively. These results suggested that the 11.42° clay angle model, where the clay follows the topography and the 13.34° clay angle model may be more representative of the true geological structure. This provides further evidence that the post-failure bathymetry does not represent the exact failure surface of the Verdal Port slide, as there has likely been some degree of immediate post-failure settlement of landslide debris. The 11.42° SBTnm model has therefore been interpreted as the best representation of the real soil profile, as it indicated an undrained soil strength ratio closer to what we would expect, while also correlating well with the post-failure bathymetry, after immediate settlement after slope failure is considered.

When conducting slope stability back analyses, it is often required to make an estimate of the failure surface location based on the post-failure morphology of the slope. However, this introduces significant uncertainty to the back analysis method, as it is difficult to quantify the degree of immediate settlement which has buried the true landslide slip surface. In the case of the Verdal Port slide, this was even more challenging due to the shallow marine setting in which the landslide occurred. In addition, there was a four-day delay in obtaining bathymetric data after the landslide had occurred, which further increased this source of uncertainty.

6. Conclusion and Limitations

6.1 Conclusion

This investigation has highlighted the high degree of uncertainty associated with using CPTU measurements to perform slope stability analyses. It is clearly indicated by this investigation that in such complex interbedded sediments, such as those encountered at Verdal Port, the interpretations of thickness, horizontal continuity and soil type can all be highly variable depending on which SBT classification scheme is used to interpret the stratigraphy. The complex, heterogeneous nature of the deltaic sediments encountered in Verdal Port, in combination with these uncertainties associated with CPTU measurements probably played a major role in the original misinterpretation of the Verdal Port sediments which resulted in the overestimation of the Verdal Port slope's factor of safety, ultimately leading to the initiation of the Verdal Port landslide.

The soil profiles produced by each of the SBT, SBTn and SBTnm charts were all significantly different, particularly with respect to the weak and sensitive clay layer which is a fundamental component for the slope stability analysis at Verdal Port. The SBT classification indicates there is sensitive fine-grained material extending from CPTU 1 past CPTU 2, while SBTn and SBTnm classifications indicate sensitive fine-grained soil at CPTU 1 but terminating before CPTU 2 with thicknesses at CPTU 1 of 2 cm and 38 cm, respectively. In contrast, the SBTn B_q chart used in (Moholdt, 2019) indicated that clay layers are present, although there is an absence of soils classified as sensitive fine-grained.

The SBTnm classification has been determined to be the most reliable as it uses more reliable pore pressure parameters, accounts for microstructural influence and gives the best indication of the soil behaviour at large strains (Robertson, 2016). In addition, the PLAXIS 2D modelling shows that the SBTnm model provides the best fit when comparing the suggested landslide failure mechanism to the post-failure bathymetry. As the SBTnm profile has been determined as most likely representing the actual geological structure at Verdal Port, the following discussion will be based on the SBTnm models.

The finite element modelling and planar morphology of the landslide scar have confirmed that the Verdal Port landslide was a translational planar landslide that initiated as a result of the shear stress imposed by the construction of the fill, which was in exceedance of the S_u of the weak layer of clay.

The correlation between the failure mechanism suggested by the finite element model, and the post-failure bathymetry suggested that the weak clay layer does not extend to CPTU 2, but instead terminates near x = 124. The limit equilibrium slope stability back analysis, for the SBTnm model with a clay layer angle of 11.42° indicated required S_u values of 6.58 kPa at high tide and 6.61 kPa at low tide in order to achieve a factor of safety equal to one. This corresponded to an undrained soil strength ratio of 0.18 – 0.20, which is in line with the lower limit of what we would expect based on (Jamiolkowski et al., 1985). Therefore, the x = 124 SBTnm model, with the clay layer angle of 11.42° has been determined as the best fitting model as it correlated well with the post-failure bathymetry, after accounting for immediate settlement and also provided a feasible undrained soil strength ratio.

The delay in failure, where the landslide occurred after fill construction had ceased for the day, may have been due to tidal fluctuation. This is suggested because the tidal modelling of the

best fit model indicates that the stability of the slope decreases with the lowering of the water level. The tidal data from 8th January 2019 support this theory as high tide occurred at 1:03 pm and low tide at 7:16 pm so therefore the FS would have been decreasing until a minimum at 7:16 pm, at which time it is likely all work had finished for the day.

The investigation into the effects that the weak clay layer's thickness and angle have on slope stability further highlighted the uncertainty associated with conducting slope stability analysis solely based on CPTU data, as changes in thickness and angle of the weak layer have a great impact on the overall stability of the slope.

There is significant evidence that suggests the weak, sensitive clay layer in which the Verdal Port landslide initiated is associated with an event bed formation. The deposition of this clay-rich layer was probably due to an abrupt increase in fine material in the Verdal River following terrestrial quick clay landslides along the river. This fine material then flowed downstream and deposited rapidly as deltaic Verdal Port sediments. Evidence of this mode of deposition includes:

- Several large quick clay landslide failures in the Trondheim region that have been well documented (L'Heureux et al., 2009). Including the 1893 Verdal landslide, which occurred up the Verdal River.
- Event beds are commonly associated with submarine slope failures throughout Norwegian fjords. These have been identified at the nearby Nidelva river delta and are known to have a regional extent (L'Heureux et al., 2011).
- Failure through such event beds typically produces translational landslides, characterised by smooth, planar rupture surfaces with distinct head scarps (L'Heureux et al., 2011). Such characteristics were observed for the Verdal Port landslide.
- Clay-rich event bed layers are generally softer and more sensitive than surrounding sediments (Hansen et al., 2011, L'Heureux et al., 2012), as is interpreted in the Verdal Port failure layer.
- The weak clay layer's locality, depth and local sedimentation fit roughly with the timeframe of the 1893 Verdal landslide (Moholdt, 2019).

Building on previous studies from (L'Heureux et al., 2009), (Hansen et al., 2011) and (L'Heureux et al., 2012) this paper has further highlighted the hazard that weak clay layers formed during event bed deposition can present in terms of slope instability. The Verdal Port landslide provides an example of how such weak clay layers can be difficult to identify, especially in complex, heterogenous soils, such as are often encountered in deltaic environments. The Verdal Port slide also provides an example of the severe negative consequences that may arise if weak soil layers are not properly considered during geotechnical design. Therefore, in order to avoid future submarine slope failures, the information provided during this investigation should be kept in mind during future developments in Norwegian Fjords and other environments in which weak event bed formations are likely to exist.

6.2 Limitations

This investigation attempted to define a soil stratigraphy and perform slope stability back analysis based on available CPTU measurements, post-failure bathymetry, finite element modelling techniques and geotechnical knowledge. Although these techniques are powerful

tools for geotechnical investigation, to obtain a more reliable geotechnical understanding of the sediments and slope stability, further CPTU soundings, in-situ field tests and laboratory testing on satisfactory quality samples are desirable. However, in the case of the Verdal Port landslide, post-landslide conditions made these methods impossible to implement due to the displacement and destruction of the soil in question. Therefore, even though this investigation has attempted to account for several areas of uncertainty and chosen a best fit model based on the geotechnical data available, there is still a high degree of uncertainty that cannot be eliminated due to the inability to perform desired geotechnical investigations.

Sources of uncertainty include:

- CPTU thin layer and transition zone affects. Although these effects can be reduced by thin layer corrections such as the inverse filtering method by (Boulanger and DeJong, 2018), it is impossible to completely eliminate this source of error.
- Some geotechnical input parameters used in the PLAXIS 2D finite element modelling have been estimated based on geotechnical judgement and previous experience rather than direct measurements.
- The soil stratigraphy outside of the two CPTU soundings is highly uncertain and has been projected using CPTU measurements and geological and geotechnical judgement.
- Deltaic sediments are complex with an abundance of thin interlayered and discontinuous soil layers, making interpretations from CPTU data very challenging.
- The exact time of failure and tidal elevation at failure is unknown.

Although the soil has been displaced and it is impossible to perform further in-situ investigations, further investigations that could have improved the understanding of the Verdal Port slide include:

- Further CPTU soundings performed pre-failure, to get a higher resolution interpretation of the soil profile and more accurate indication of the weak clay layer termination point.
- SCPTU investigations so that presence of microstructure within the weak clay can be assessed more reliably.
- Core sampling of sediments to determine the actual soil profile. However, it may be difficult to retrieve such soft-sediment samples from the shallow marine environment.
- Sampling of weak clay layer and subsequent laboratory investigations, to identify mineralogy, organic carbon levels, bioturbation, and presence of microstructure. This could be compared to other Norwegian Fjord event bed studies to confirm event bed mode of deposition.
- Further studies into the role the thickness of a weak layer has on slope stability, with a focus on thin layers less than 10 cm.
- Further studies focusing on the geotechnical character of event bed sediments and the geotechnical variation between these and adjacent sediments. This would simplify the identification of these soils.

References

AAS, G., LACASSE, S., LUNNE, T. & HOEG, K. 1988. Use of in situ tests for foundation design on clay International Journal of Rock Mechanics and Mining Sciences & Geomechanics Abstracts, 25, A8.

AHMADI, M. M. & ROBERTSON, P. K. 2005. Thin-layer effects on the CPT qc measurement. Canadian Geotechnical Journal, 42, 1302-1317.

BÆVERFJORD, M. G. & THAKUR, V. 2008. The Verdal and Rissa Landslides-Application of case histories in education. 6th International conference on case histories in geotechnical engineering. Arlington, VA.

BJERRUM, L. 1955. Stability of natural slopes in quick clay. Geotechnique, 5, 101-119.

BOULANGER, R. W. & DEJONG, J. T. 2018. Inverse filtering procedure to correct cone penetration data for thin-layer and transition effects, The Netherlands, Delft University of Technology.

CHANDLER, R. J. 1977. Back analysis techniques for slope a case record. Geotechnique 27, 479-495.

CRUSOE-JR, G., QING-XIANG, C., JI-SEN, S., LIU1, H. & BARVOR, Y. J. 2016. Effects of Weak Layer Angle and Thickness on the Stability of Rock Slopes. International Journal of Mining and Geo-Engineering, 50, 97-110.

DOUGLAS, B. J. & OLSEN, R. S. 1981. Soil classification using electric cone penetrometer. Symposium on Cone Penetration Testing and Experience. St. Louis.

DUNCAN, J. M. & WRIGHT, S. G. 2005. Soil Strength and Slope Stability, New Jersey, John Wiley & Sons, Inc.

ESLAAMIZAAD, S. & ROBERTSON, P. K. Seismic cone penetration test to identify cemented sands. 49th Canadian Geotechnical Conference, 1996 St. John's, Newfoundland. 352–360.

FEAR, C. E. & ROBERTSON, P. K. 1995. Re-consideration of Initiation of Liquefaction in Sandy Soils. Journal of Geotechnical Engineering, 121, 249-261.

GARIANO, S. L., RIANNA, G., PETRUCCI, O. & GUZZETTI, F. 2017. Assessing future changes in the occurrence of rainfall-induced landslides at a regional scale. Science of the Total Environment, 596-597, 417-426.

GILBERT, R. B., WRIGHT, S. G. & LIEDTKE, E. 1998. Uncertainty in Back Analysis of Slopes: Kettleman Hills Case History. Journal of Geotechnical and Environmental Engineering, 124, 1167-1176.

GILLESPIED, G. 1989. Evaluating velocity and pore pressure data from the cone penetration test. Ph. D, University of British Columbia.

HAMPTON, M. A., LEE, H. J. & LOCAT, J. 1996. Submarine Landslides. Reviews of Geophysics, 34, 33-59.

HANSEN, L., L'HEUREUX, J. S. & LONGVA, O. 2011. Turbiditic, clay-rich event beds in fjord-marine deposits caused by landslides in emerging clay deposits – palaeoenvironmental interpretation and role for submarine mass-wasting. The Journal of the International Association of Sedimentologists, 58, 890-915.

HERMANNS, R., OPPIKOFER, T., ROBERTS, N. & SANDØY, G. 2014. Catalogue of Historical Displacement Waves and Landslide. Engineering Geology for Society and Territory, 4, 63-66.

HOULSBYG, G. 1988. Penetration Testing in the U.K. Birmingham.

HUNDAL, E. & ØISETH, E. 2019. Geoteknisk Vurdering for Utbygging av Verdal Havn. Ramboll Norge AS.

JAMIOLKOWSKI, M., LADD, C. C., GERMAINE, J. T. & LANCELOTTA, R. 1985. New developments in field and laboratory testing of soils. 11th International Conference on Soil Mechanics and Foundation Engineering. San Francisco, California.

JOHANSSON, J. M. A. & EDESKÄR, T. 2014. Effects of External Water-Level Fluctuations on Slope Stability. The electronic journal of geotechnical engineering, 19, 2437-2463.

L'HEUREUX, J.-S., HANSEN, L. & LONGVA, O. 2009. Development of the submarine channel in front of the Nidelva River, Trondheimsfjorden, Norway. Marine Geology, 260, 30-44.

L'HEUREUX, J.-S., HANSEN, L., LONGVA, O. & EILERTSEN, R. S. Landslides along Norwegian fjords: causes and hazard assessment. The Second World Landslide Forum, 03-07 October 2011 Rome.

L'HEUREUX, J.-S., LONGVA, O., STEINER, A., HANSEN, L., VARDY, M. E., VANNESTE, M., HAFLIDASON, H., BRENDRYEN, J., KVALSTAD, T. J., FORSBERG, C. F., CHAND, S. & KOPF, A. 2012. Identification of Weak Layers and Their Role for the Stability of Slopes at Finneidfjord, Northern Norway, Submarine Mass Movements and Their Consequences. Advances in Natural and Technological Hazards Research.

LIAN-HENG, Z., SHI, Z., YU-LIANG, L., LIANG, L. & YINGBIN, Z. 2016. Reliability back analysis of shear strength parameters of landslide with three-dimensional upper bound limit analysis theory. Landslides, 13, 711-724.

LIU, Z. & KOYI, H. 2013. The impact of a weak horizon on kinematics and internal deformation of a failure mass using discrete element method. Tectonophysics, 586, 95-111.

LUNNE, T., ROBERTSON, P. K. & POWELL, J. J. M. 1997. Cone Penetration Testing in Geotechnical Practice, London, U.K.

MOHOLDT, R. 2019. Verdal Havn. Undersjoisk Skred. Tredjepartskontroll. NGI Teknisk Notat.

PLAXIS 2018. PLAXIS 2D Reference Manual.

ROBERTSON, P. K. 1990. Soil classification using the cone penetration test. Canadian Geotechnical Journal, 27, 151-158.

ROBERTSON, P. K. 2010. Soil behaviour type from the CPT: an update. 2nd International Symposium on Cone Penetration Testing.

ROBERTSON, P. K. 2016. Cone penetration test (CPT)-based soil behaviour type (SBT) classification system — an update. Canadian Geotechnical Journal, 53, 1910-1927.

ROBERTSON, P. K., CAMPANELLA, R. G., GILLESPIE, D. & GREIG, J. 1986. Use of Piezometer cone Data. ASCE Specialty Conference.

SCHNAID, F. 2009. In-situ testing in geomechanics – the main tests, London, Taylor & Francis Group.

SCHNEIDER, J. A. & MOSS, R. E. S. 2011. Linking cyclic stress and cyclic strain based methods for assessment of cyclic liquefaction triggering in sands. Geotechnique Letters.

SCHNEIDER, J. A., RANDOLPH, M. F., MAYNE, P. W. & RAMSEY, N. R. 2008. Analysis of factors influencing soil classification using normalized piezocone tip resistance and pore pressure parameters. Journal of Geotechnical and Geoenvironmental Engineering Geology for Society and Territory, 134, 1569–1586.

SCHUSTER, R. L. 1996. Socioeconomic significance of landslides. Landslides: Investigation and Mitigation, 247.

SERGEYEV, Y. M., GRABOWSKA-OLSZEWSKA, B., OSIPOV, V. I., SOKOLOV, V. N. & KOLOMENSKI, Y. N. 1980. The classification of microstructures of clay soils. The Journal of Microscopy, 120.

TREADWELL, D. D. 1976. The influence of gravity, prestress, compressibility, and layering on soil resistance to static penetration. Ph. D, The University of California.

WROTH, C. P. 1984. Interpretation of In situ soil test. Geotechnique, 34, 449-489.

YAMADA, Y., KAWAMURA, K., IKEHARA, K., OGAWA, Y., URGELES, R., MOSHER, D., CHAYTOR, J. & STRASSER, M. 2012. Submarine Mass Movements and their Consequences - 5th International Symposium. Advances in Natural and Technological Hazards Research, 31, 1-12.

Appendix A - SBTnm Failure Mechanisms

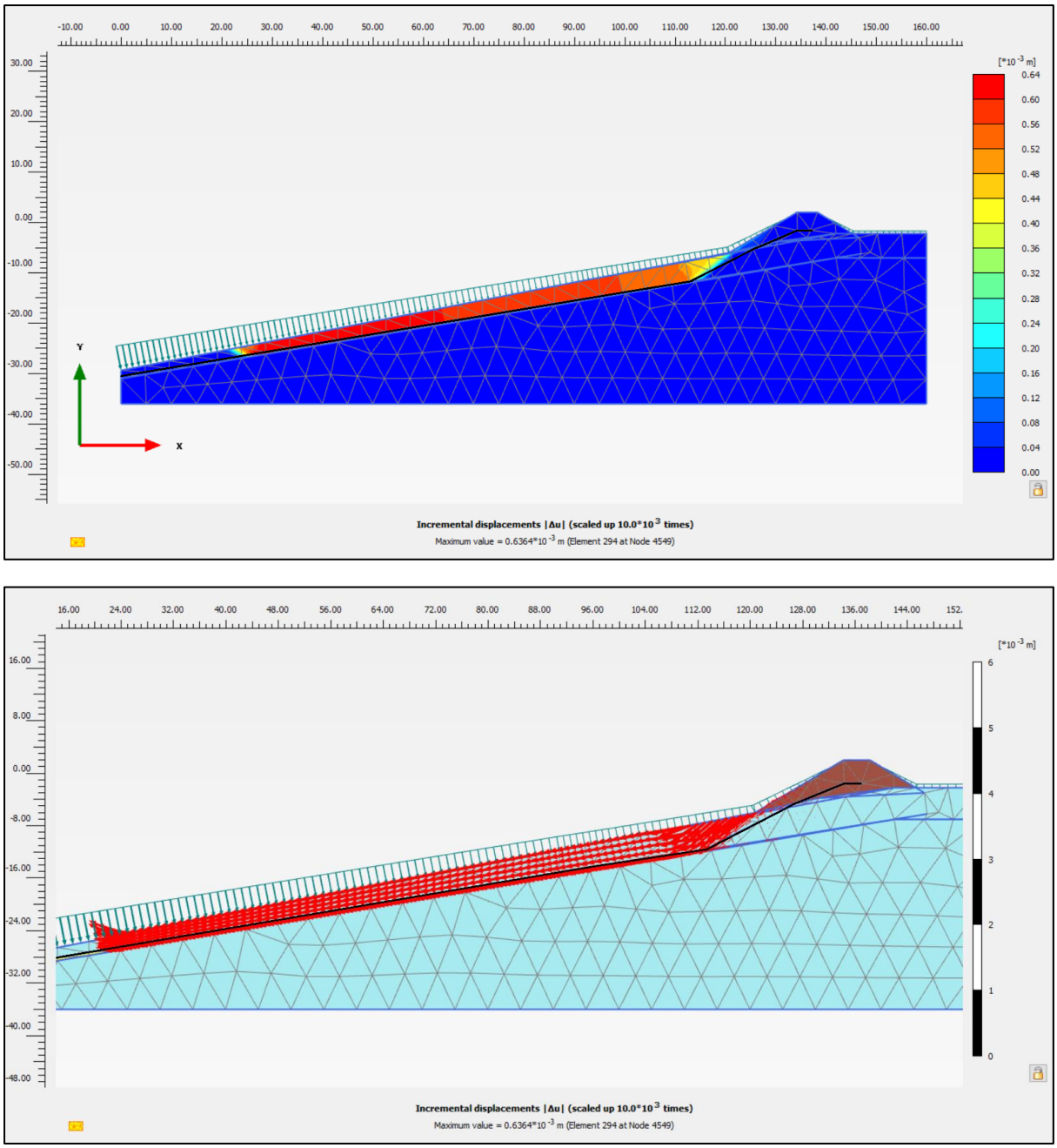

Figure A.1: Incremental displacement plots for clay layer pinching before CPTU 2 at x =117, (SBTnm Profile). Post-failure terrain is indicated by the black line.

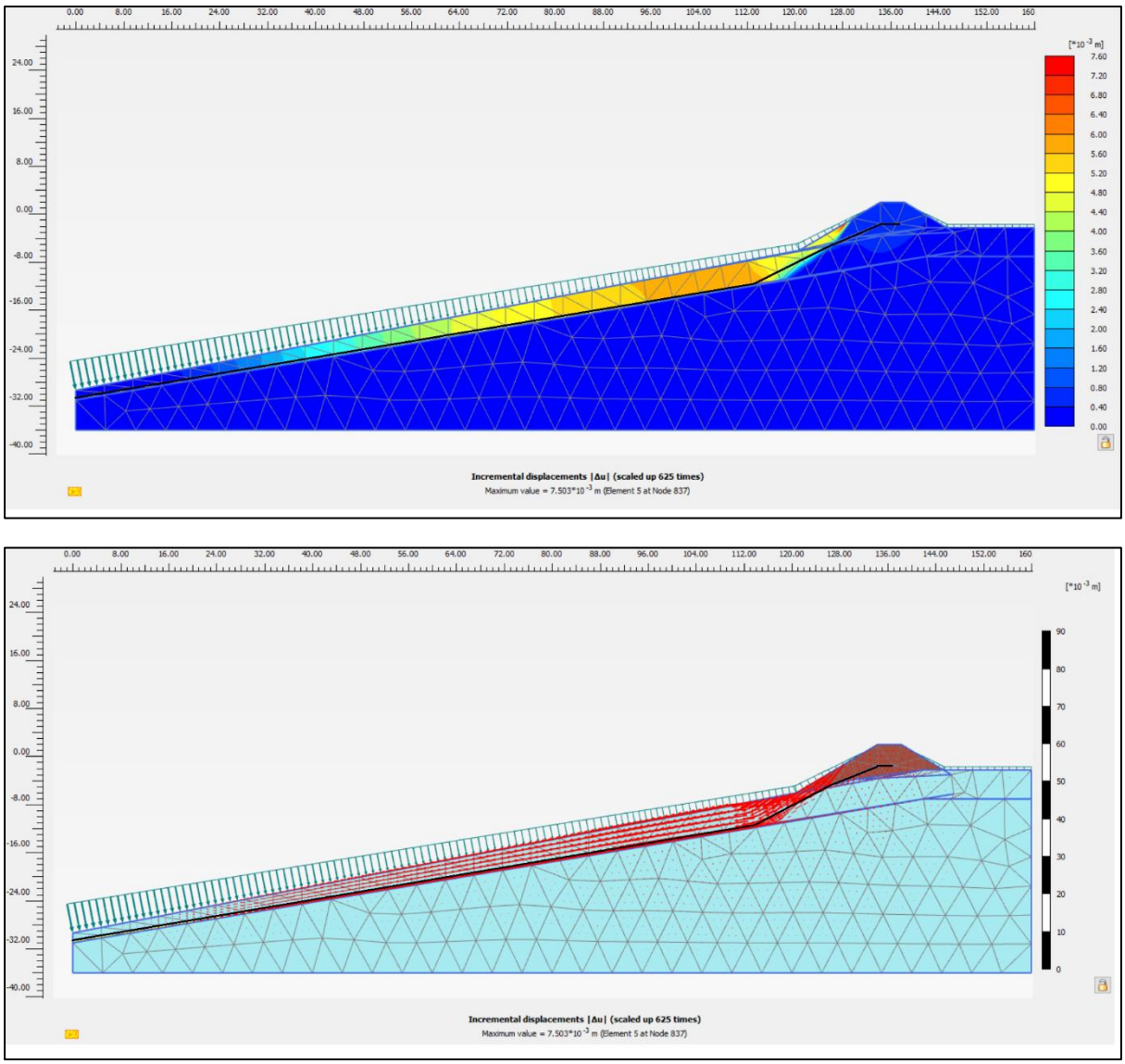

Figure A.2: Incremental displacement plots for clay layer pinching before CPTU 2 at x =119, (SBTnm Profile). Post-failure terrain is indicated by the black line

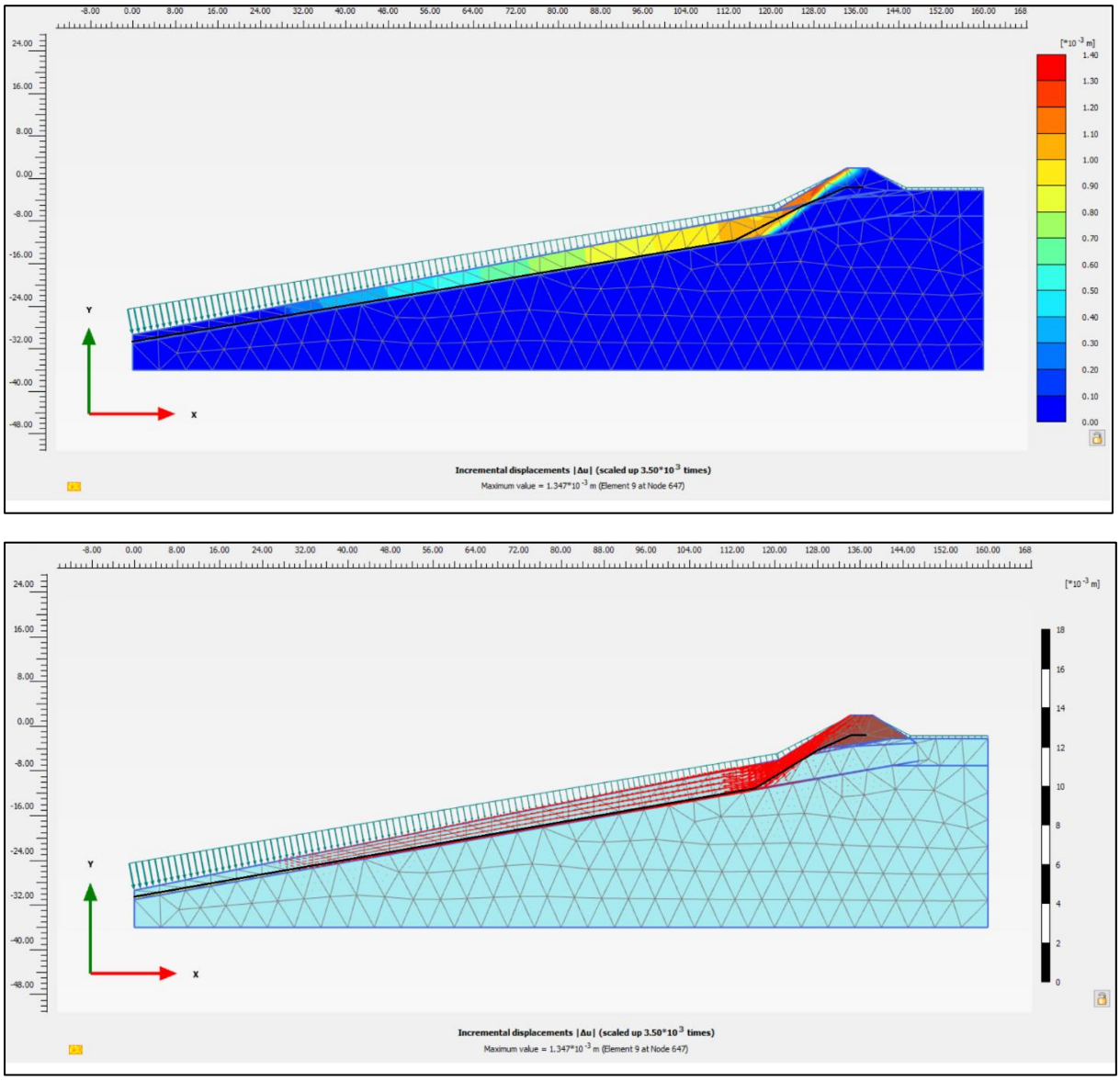

Figure A.3: Incremental displacement plots for clay layer pinching before CPTU 2 at x =121, (SBTnm Profile). Post-failure terrain is indicated by the black line

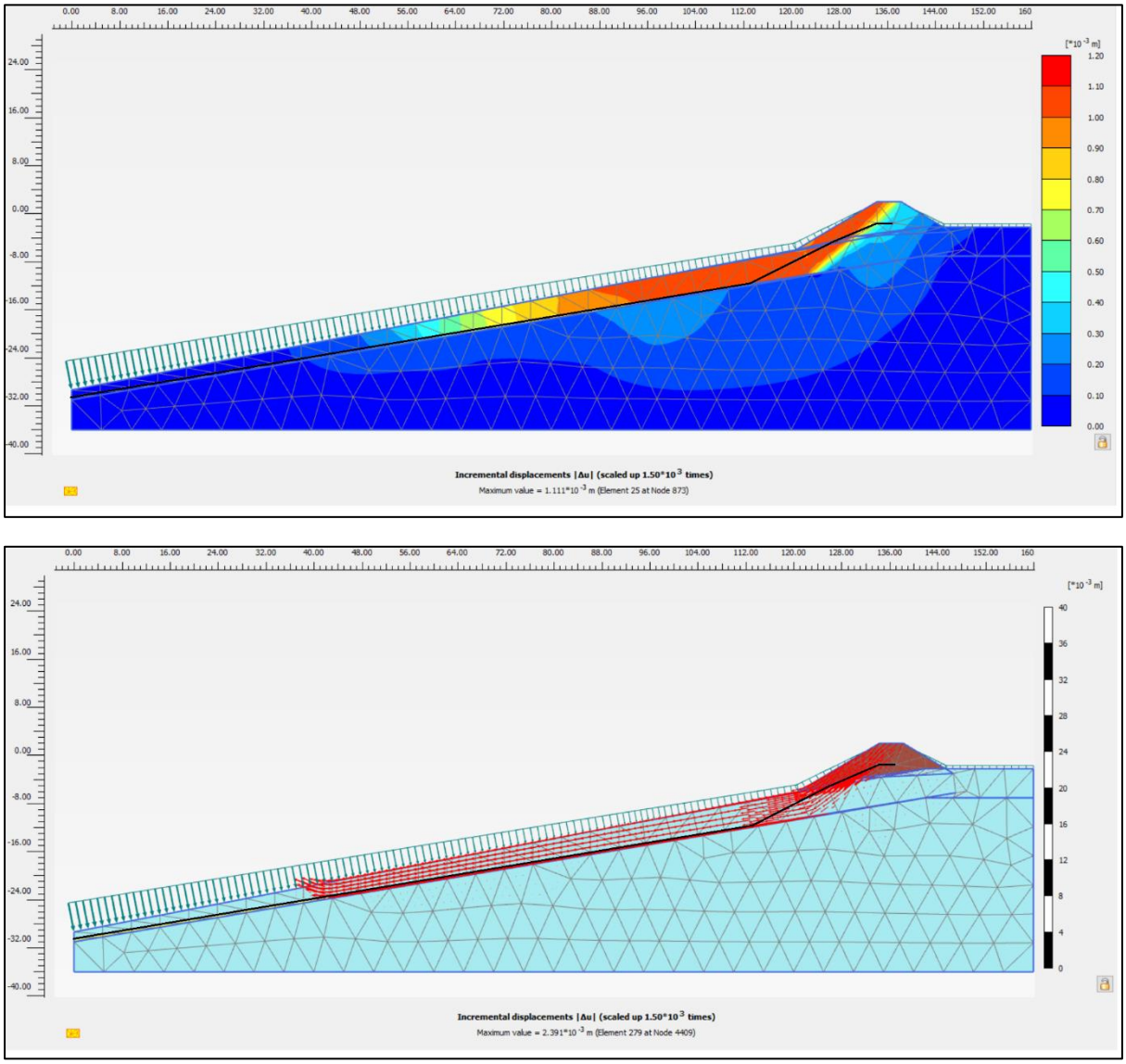

Figure A.4: Incremental displacement plots for clay layer pinching before CPTU 2 at x =126, (SBTnm Profile). Post-failure terrain is indicated by the black line

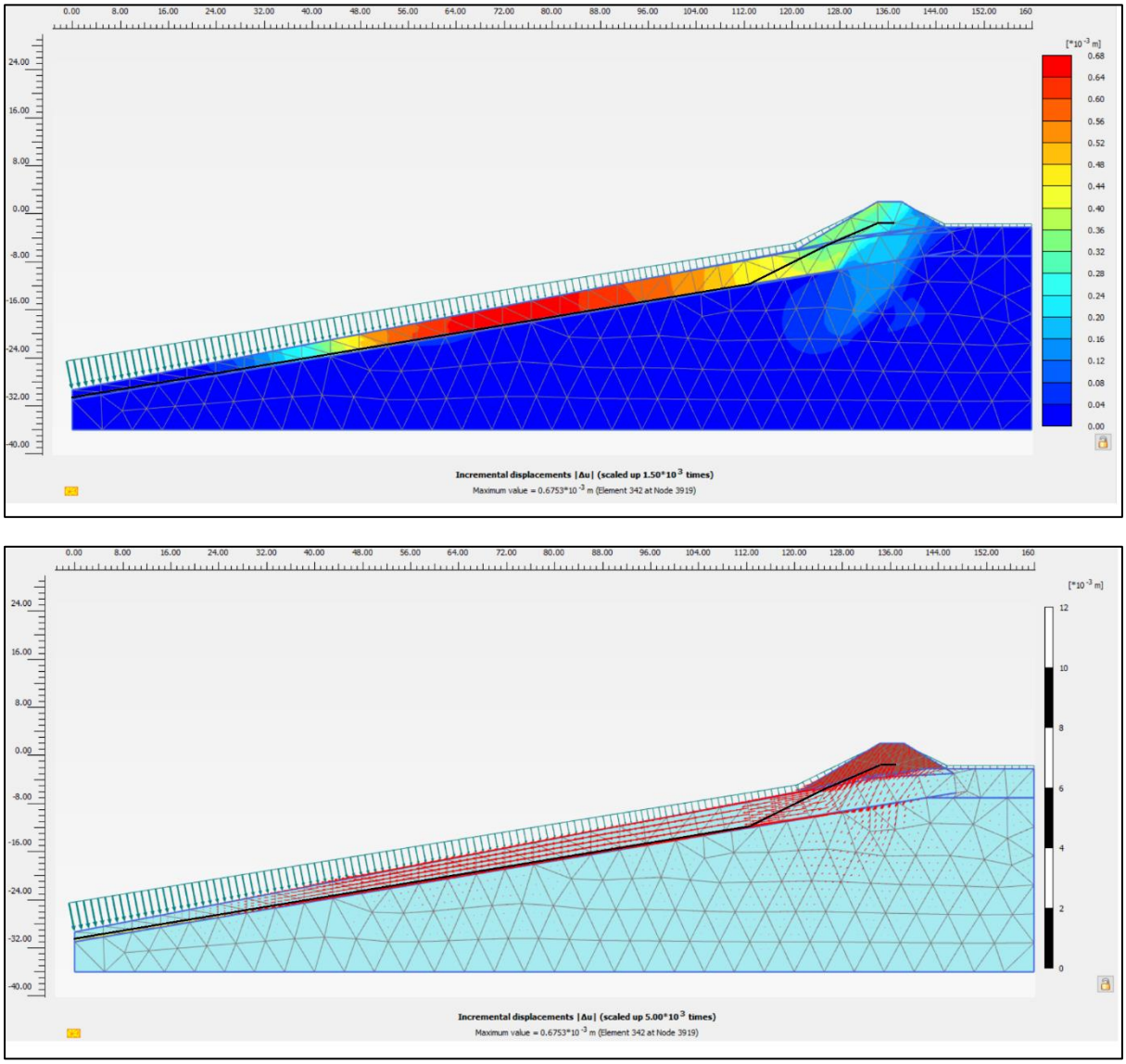

Figure A.5: Incremental displacement plots for clay layer pinching before CPTU 2 at x =128, (SBTnm Profile). Post-failure terrain is indicated by the black line